Geology, mineralogy, ore paragenesis, and molybdenite Re-Os geochronology of Sn-W (-Mo) mineralization in Padatgyaung and Dawei, Myanmar: Implications for timing of mineralization and tectonic setting

Aung Zaw Myint[1, 2*], Huan Li[3*], Andrew Mitchell[4], David Selby[5, 6], Thomas Wagner[2]

[1]Department of Geology, University of Yangon, Yangon, Kamayut 11041, Myanmar

[2]Institute of Applied Mineralogy and Economic Geology, RWTH Aachen University, Wüllnerstr. 2, D-52062 Aachen, Germany

[3]Key Laboratory of Metallogenic Prediction of Nonferrous Metals and Geological Environment Monitoring, Ministry of Education, School of Geosciences and Info-Physics, Central South University, Changsha 410083, China

[4] 20, Dale Close, Oxford OX1 1TU, United Kingdom

[5]Department of Earth Sciences, University of Durham, Durham, DH1 3LE United Kingdom

[6]State Key Laboratory of Geological Processes and Mineral Resources, China University of Geosciences, Wuhan 430074, China

Date: 19 August 2020

Resubmission date: 09 February 2021

Resubmission date: 20 February 2021

[*]corresponding author:

AZM: aungzawmyint.myanmar@gmail.com

HL: lihuan@csu.edu.cn

Abstract

The Sn-W (-Mo) deposits of Myanmar are mostly located in the Western Granite Province that is well known for its world-class Sn-W (-Mo) deposits. Previous studies have constrained the age of the granitic intrusions of the province and the timing of mineralization for a few deposits, but most of the mineralization ages are not well established. In this study, new molybdenite Re-Os dating of two Sn-W-(Mo) regions, Padatgyaung and Dawei, together with their geological setting and mineral paragenesis are carried out to constrain the timing of ore formation and geodynamic setting. In the Padatgyaung region, two weighted average Re-Os model ages of 64.23 ± 0.29 Ma (MSWD = 0.49, 2σ) and of 60.54 ± 0.45 Ma (MSWD = 1.3, 2σ) from vein molybdenites are considerably younger than molybdenite from tin mineralized greisen which has a weighted Re-Os model age of 68.5 ± 2.7 Ma (MSWD = 0.14, 2σ). This demonstrates that the vein-type W-Mo mineralization formed after tin mineralized greisenization. Combining our new age data with previous geochronological data, the Re-Os model age of 63.09 ± 0.17 Ma from the Wagone quartz vein suggests that the Sn-W(-Mo) mineralization in the Dawei region took place at around 70-60 Ma (Late Cretaceous to Paleocene). This study indicates the presence of a significant and discrete granite-related Sn-W(-Mo) mineralization with an age of 75-60 Ma in the Western Granite Province, although the overall age range of Sn-W mineralization in the belt spans from 120 to around 40 Ma emplaced during normal subduction and roll-back of the Neo-Tethyan oceanic crust.

Keywords: Re-Os geochronology; Sn-W (-Mo) deposits of Myanmar; Western Granite Province; Late Cretaceous to Paleocene event

1. Introduction

Myanmar is a major tin and tungsten producer with about 400 known individual Sn-W deposits, prospects, and occurrences which form an approximately N-S trending belt (e.g., Than Htun et al., 2017). Together, they form a significant part of the Southeast Asia Tin Belt and makeup about 5% of the world's tin reserves (ITRI, 2016) and about 17% of the world's tin production (Lehmann, 2000). The Sn-W-Mo mineralization predominantly occurs as quartz veins, greisens, pegmatites, and skarns, geologically and genetically associated with the granitic rocks of the Western and Central Granite Provinces (Mitchell, 1977; Cobbing et al., 1986, 1992). The Cretaceous to Eocene granites of the Western Granite Province were emplaced along the western margin of the Sibumasu terrane and host hundreds of Sn-W occurrences located in Myanmar and Southwest Thailand, including the large Sn-W deposit at Mawchi (Hobson, 1940; Khin Zaw and Khin Myo Thet, 1983; Aung Zaw Myint et al., 2017b, 2018). This granite belt reappears in the Tengchong terrane in China in the north, where it hosts some Sn-W deposits, including the important Xiaolonghe and Lailishan deposits (Chen et al., 2015; Cao et al., 2019) (Fig.1).

The Padatgyaung and Dawei Sn-W regions of Myanmar comprise a number of Sn-W (-Mo) prospects with diverse styles of mineralization. Systematic lode tin mining has been developed only at a few localities, all in the Dawei region, although historical records indicate that tin has been found and mined a few hundred years in these two regions. The long history of mining, although without any systematic production record, illustrates that the deposits described in this study are of considerable economic significance. In recent years, the timing of ore formation in these two regions, especially in Dawei, has been established based on geological observations and geochronological dating of the host granites (Gardiner et al., 2016; Jiang et al., 2017; Li et al., 2018a, 2018b), but direct age dating of the Sn-W deposits is still required in order to understand the timing of Sn-W-Mo mineralization and the temporal relations with the emplacement of the associated different types of granitic intrusions. In order to address this question, this study provides geology, mineralogy, ore deposit characteristics, and new molybdenite Re-Os ages of mineralizations from the Padatgyaung and Dawei regions to constrain the nature, timing, and tectonic setting of Sn-W (-Mo) mineralization in two Sn-W regions of Myanmar.

2. Geological background

2.1 Regional geology

The Western Granite Province (Cobbing et al., 1986, 1992) of SE Asia contains several generations of I- and S-type granites of Jurassic to Miocene age (Khin Zaw, 1990; Cobbing et al., 1992; Barley et al., 2003; Searle et al., 2007; Mitchell et al., 2012; Gardiner et al., 2016, 2018; Aung Zaw Myint et al., 2017a,2017b; Crow and Khin Zaw, 2017; Li et al., 2018a, 2018b, 2019) intruding the metamorphic rocks of the Mogok Metamorphic Belt (MMB; Searle and Haq, 1964; Mitchell et al., 2007) and the sedimentary rocks of the Mergui-Mawchi Belt, formerly termed as Slate Belt (Mitchell et al., 2004) (Fig. 1B). The MMB formed as a western margin of the Sibumasu terrane, comprising a metasedimentary and metaigneous sequence of marbles, calc-silicate rocks, schists, quartzites, gneisses, and migmatites (Searl and Haq, 1964; Mitchell et al., 2007). The Mergui-Mawchi Belt comprises Carboniferous to Early Permian glacio-marine diamictites, including sedimentary rocks and their metasedimentary equivalents classified as Mawchi, Lebyin, Taungnyo, and Mergui Groups in Myanmar, as Kaeng Krachan and Phuket Groups in Thailand, and probably as Kongshuhe Formation in western Yunnan. The Sn-W(-Mo) mineralization is spatially and genetically related to the Mawchi-Mergui Belt-hosted peraluminous granitic rocks in the Western Granite Province.

Jurassic biotite granites (with ages of around 180 Ma) in the Western Granite Province exposed at Mangzhangxiang (Yunnan) and Taunggwa (Myanmar) are metaluminous, I-type in geochemical character and tin-barren. They are enriched in large-ion lithophile elements coupled with depletion in high field strength elements (Crow and Khin Zaw, 2017; Cao et al., 2018) and not associated with Sn-W mineralization. The Cretaceous granitoids (121-68 Ma) include both metaluminous, sodic-potassic magnetite-series I-type granitic to dioritic rocks occurring in the Laochasnpo and Guyong (Yunnan), Yebokeson, Yinmabin, and Mokpalin area (Myanmar), and peraluminous S- and A-type tin granites exposed at Dabinga and Xiaolonghe (Yunnan), Nattaung, Mawpalaw Taung, Tagu, and Hermyingyi (Myanmar), and Pilok (Thailand) (Fig. 1B) (Charusiri et al., 1993; Barley et al., 2003; Mitchell et al., 2012; Crow and Khin Zaw, 2017; Mi Paik, 2017; Jiang et al., 2017; Zhao et al., 2017; Cao et al., 2019; Kyaw Thu Htun et al., 2019; Cong et al., 2020; Mao et al., 2020). Younger Paleocene to Eocene (about 65-40Ma) granitoids consist of metaluminous to mildly peraluminous, high-K calc-alkaline granitoid series that contain highly fractionated S- and A-type granitic rocks with Sn-W mineralization in the Lailishan (Yunnan), Padatgyaung, Hermyingyi, Wagone, Yadanapon, and Mawchi area (Myanmar) (Brook and Snelling, 1976; Chen et al., 2015; Aung Zaw Myint et al., 2017a, 2017b) as well as tin-barren I-type granites in Kyaikhtiyo and Tawmoe Taung (Mitchell et al., 2012; Crow and Khin Zaw, 2017). The youngest Miocene S- and I-type granitoids (30-15) exposed at Kyanigan, Yesin Dam, Payangazu, and Kabaing (Searle et al., 2007; Mitchell et al., 2012; Crow and Khin Zaw, 2017) are not associated with any Sn-W mineralization.

2.2 Padatgyaung W-Sn (-Mo) Region

The W-Sn (-Mo) deposits in the Padatgyaung region are confined to a partly weathered and greisenized biotite granite, which has intruded the low-grade metasedimentary rocks of the Mawchi Group (Fig. 2). The granite and metasedimentary rocks are bounded by the medium- to high-grade metamorphic rocks of the MMB to the west and Cambrian to Cretaceous sedimentary rocks of Shan Plateau to the east. Banded gneisses, schists, marbles, and calcsilicate rocks are part of the lithologic units of the MMB in this region. The granite is exposed as a north-south elongate pluton comprising medium- to coarse-grained quartz, orthoclase, plagioclase, biotite, and muscovite. Biotite occurs as the major mafic mineral occupying about 10% of the rock volume, being partially chloritized. The muscovite content is less than 3 vol% but increases up to 35 vol% in the greisenized parts (Aung Zaw Myint et al., 2019). Granites and greisens from Padatgyaung have 19 ppm – 9 wt.% Sn, 15 ppm – 0.5 wt.% W and 10 – 186 ppm Mo. The granite is silica rich (74-77 wt.% SiO_2), geochemically highly evolved, and peraluminous (Aung Zaw Myint et al., 2019). Granite samples have low Zr concentrations, reflecting low temperatures of crystallization and high-level emplacement (Kalsbeek et al., 2001; Aung Zaw Myint et al., 2017b). MORB-normalized spider diagrams of the granites show enrichment in LILE, such as U, Th, and Rb, with distinct negative anomalies for the HFSE Ti and Nb (Aung Zaw Myint et al., 2019). These geochemical features are characteristic for granites formed from typical crustal melts (e.g., Harris et al., 1986). Biotite K-Ar dating of the granites close to Padatgyaung and Pyiyadana yielded ages of 55±1 Ma and 57±1 Ma, respectively (Brook and Snelling, 1976). Greisenization, the product of magmatic-hydrothermal alteration, occurs pervasively in the host rocks, and appears to be coeval with pre- and syn-veining post-magmatic fluid flow focusing along the NE-SW, N-S, and WSW-ENE trending fractures.

Bateson et al. (1972) first reported that the Padatgyaung granite hosts several Sn-W deposits which contain wolframite and lesser amounts of cassiterite, associated with minor chalcopyrite, galena, pyrite, scheelite, monazite, and ilmenite in quartz veins and greisen zones. They focused on the Sn-W deposits located at the western margin of the granite, whereas the molybdenite bearing Sn-W deposits at the eastern margin were not investigated.

The W-Sn-Mo mineralization at Padatgyaung comprises two types of mineralization: (i) Sn-rich greisen type and (ii) W-rich quartz vein type. Generally, the prospects in the northern part of the region represent the Sn-rich greisen type (e.g., Pyiyadana, Bularmi), whereas those in the southern part are W-rich quartz veins (e.g., Tayokegone, Shwechaung, Tagun Taung). The Sn-rich greisen mineralization in Pyiyadana occurs mainly as the greisen style forming irregular patches (Fig. 3A) and veins in the greisenized granite and sedimentary rocks. The greisen contains a considerable amount of molybdenite, cassiterite, fluorite, and rare sulfides. Numerous small greisen-bordered quartz veins trend WNW-ESE and discordantly cut the mudstones (Fig. 3B). Most veins strike approximately north-south and dip sub-vertically (80-90°). The vein thickness ranges from 1 m to 9 m and the greisenized zone has an orientation with a strike of NNE-SSW in Pyiyadana. To the south, some Sn-W bearing greisen veins are hosted by partly altered mudstone and conglomeratic mudstone. The Sn-W minerals occur as disseminated grains in the greisen veins, which generally trend 130° and dip to the SW. The major ore minerals in these veins are cassiterite and wolframite, associated with minor amounts of scheelite, arsenopyrite, pyrite, chalcopyrite, sphalerite, bornite, and galena. More detailed geological observations are precluded by a thick cover of soil and dump material originating from artisanal placer mining over a wide area encompassing the Bularmi, Akaung Taung, and Seikphu Taung prospects. Narrow exposures in an adit show that the quartz veins are greisen-bordered and contain cassiterite, wolframite, pyrite, and chalcopyrite as the main ore minerals (Fig. 3C).

The second type of mineralization is W-rich quartz veins. Wolframite-bearing quartz veins at Tayokegone (Fig. 3D) contain minor amounts of sulfides such as molybdenite and pyrite and these veins are confined to the metasediments. The Shwechaung, Sakangyi, and Myinmahti prospects surround the peak of Myinmahti hill, the highest peak of the region with an elevation of 1243 m above sea level. The N-S trending wolframite-bearing quartz veins are

0.12 to 0.25 m thick and crosscut the greisenized granite at Sakangyi. The veins taper downwards and contain irregular patches and fracture fillings of wolframite. At Shwechaung, the moderately inclined wolframite and molybdenite bearing quartz veins strike in a NNE-SSW direction and cut the greisenized granite. The veins are 0.9 to 2.1 m thick and contain wolframite, molybdenite (Fig. 3E), galena, pyrite, chalcopyrite, and sphalerite. Sulfide minerals occur as disseminated and irregular patches in the quartz veins. The steeply dipping to sub-vertical veins at Myinmahti have a generally NNE-SSW strike with widths ranging from a few centimeters to several meters. By contrast, a different set of E-W trending veins is barren. The greisenized zone with irregular shape and variable thickness hosts the mineralized quartz veins (Fig. 3F). Common ore minerals in the veins include wolframite, cassiterite, molybdenite, and pyrite. These ore minerals also form the major constituents of the greisenized zone, which additionally contains quartz and muscovite. At Yadana Gadaytike, the vein system comprises about 15 essentially subparallel mineralized quartz veins that cut the N-S margin of the weathered granite, forming the southernmost Sn-W prospect of the region. The veins are greisen-bordered, slightly weathered, and carry wolframite with minor cassiterite (Fig. 3G). Their thickness ranges from 0.12 to 0.6 m. At the Tagun Taung prospect, quartz veins penetrate the highly weathered granite that is extensively greisenized and capped by metagreywacke. The quartz veins trend NE-SW and contain a considerable amount of molybdenite, pyrite, and wolframite, occurring as irregular patches and disseminated grains in the quartz veins, which range in width from 0.1 to 0.25 m. The syn-vein greisenization is noticeable in hand specimens (Fig. 3H).

2.3 Dawei Sn-W (-Mo) region

The Western Granite Province of SE Asia is exposed in three granite ranges in the Dawei region, namely the Coastal Range, Central Range, and Frontier Range (Brown and

Heron, 1923) (Fig. 4). They form NNW-SSE trending elongated bodies in a structural zone parallel to the regional strike of the (meta)sedimentary rocks of the Mergui Group. The Coastal Range is mainly built up of biotite granites with minor amounts of hornblende bearing granodiorite. These tin-barren granitic rocks contain mafic xenoliths up to 40 cm in diameter (Aung Zaw Myint, 2019). The northeastern part of the Coastal Range is composed of medium- to coarse-grained aplogranite and spatially associated with Sn-W occurrences, including Kanbauk and other small prospects (Aung Zaw Myint, 2019). The primary mineralization at Hermyingyi, Wagone, Bawapin, Pagaye, Pulatto, and Kalonta, and the fossil tin placer deposit at Heinda are located in the Central Range (Clegg, 1944; Aung Zaw Myint et al., 2014), where biotite and two mica granites host most of the Sn-W mineralization. There are four types of Sn-W-Mo mineralization occurring in this region, such as greisens (e.g., Bawapin), pegmatites (e.g., some veins of Bawapin), quartz veins (e.g., Putlatto, Hermyingyi, Wagone), and skarns (e.g., Kanbauk).

In the southernmost part of the Dawei Sn-W region, steeply-dipping greisen-bordered quartz veins at Putlatto are confined to a biotite granite and the metasedimentary rocks (Fig. 5A). The veins trend along a nearly N-S direction and have thicknesses of 0.5 to 3 m. The quartz veins carry wolframite, cassiterite, molybdenite, pyrite, chalcopyrite, sphalerite, and secondary covellite. The hydrothermal alteration associated with the Putlatto W(-Sn) mineralization consists of greisenization, silicification, argillic alteration, and chloritization (Ye Zaw and Aung Zaw Myint, 2018). The Heinda mine, which is the biggest tin placer (fossil placer) deposit of the region, is located in the drainage area between the Central Range granites and Mergui Group to the west. The Heinda placer deposits form a thick sequence of cassiterite bearing sediments, particularly in the Heinda Chaung, Shwe Chaung, and Hpolon Taung areas (Clegg, 1944; Nandar Oo, 1980).

The Sn-W veins at Hermyingyi are greisen-bordered and vary widely in thickness ranging from 2 cm to 3 m (Fig. 5B). A N-S trending system of sub-parallel veins dipping sub-vertically penetrates a biotite granite and the surrounding metasediments. The main ore minerals are wolframite, cassiterite, pyrite, chalcopyrite, molybdenite, sphalerite, galena, boulangerite, covellite, bismuthinite, pyrrhotite, colusite, and enargite, whereas quartz, lepidolite, fluorite, garnet, chlorite, and sericite are the dominant gangue minerals (Nilar Shwe, 1981). LA-ICP-MS U-Pb dating of zircon from the biotite granite at Hermyingyi yielded concordant U–Pb ages of 61.44 ± 0.6 Ma (MSWD = 0.9; Li et al., 2018a) and 70.44 ± 0.4 Ma (MSWD = 0.9; Jian et al., 2017), respectively. The molybdenite Re-Os isochron date indicates an age of 68.4±2.5 Ma (MSWD=0.18, 2σ) (Jiang et al., 2019) for the Sn-W-Mo vein formation at Hermyingyi. The small biotite granite stock to the south is exposed at Taungphila, where greisen-bordered quartz veins carry a considerable amount of cassiterite and wolframite. This granite has been dated as 68.8 ± 0.1 Ma (MSWD = 0.1; Jian et al., 2017) by the LA-ICP-MS U-Pb zircon dating method.

The tin granites from Hermyingyi and Wagone are high in SiO_2 (75.15–82.53 wt.%) and total alkalis (3.70 to 9.08 wt.%), but low in FeO (0.57–3.45 wt.%), CaO (0.23–0.86 wt.%), MgO (0.02–0.19 wt.%), MnO (0.01–0.38 wt.%), TiO_2 (0.01–0.10 wt.%) and P_2O_5 (0.003–0.012 wt.%). They show some variation in the MgO (0.02–0.03 wt.%), TiO_2 (0.01–0.03 wt.%) and P_2O_5 (0.008–0.012 wt.%) contents (Li et al., 2018a). These granites are metaluminous to weakly peraluminous with their primitive mantle-normalized multi-element diagrams characterized by enrichment in Rb, Th, U, Ta, and Y but strong depletion in Ba and Sr.

The Sn-W mineralization at Wagone represents a combination of W-Mo (-Sn) quartz veins and tin-rich hydrothermally altered granite (Aung Zaw Myint, 2015). Mineralized quartz veins crosscut both the granite and the metasedimentary host rocks, which strike N-E to NE-SW and dip with 50-90˚ to the west. Quartz veins trending NNW-SSE are not economic and contain only trace amounts of wolframite and cassiterite (Fig. 5C). In places, barren N-S trending quartz veins crosscut the biotite granite and host locally abundant cassiterite and wolframite. Cassiterite and magnetite are widely disseminated in the altered muscovite granite and form pinkish to reddish brown patches with up to 8 wt.% Sn (Fig. 5D). Apart from the tin-rich zone, a wolframite bearing quartz vein system is confined to a weathered biotite granite and is associated with minor amounts of platy or massive molybdenite (Fig. 5E) and rare cassiterite (Aung Zaw Myint, 2015; Aung Zaw Myint et al., 2017a). Previous LA-ICP-MS U-Pb zircon dating of the biotite granite and muscovite granite at Wagon yielded virtually identical ages of 61.4 ± 0.5 Ma (2σ, n=20, MSWD=3.0) and 60.7 ± 3.5 Ma (2σ, n=10, MSWD=7.0), respectively (Li et al., 2018a).

The Bawapin Sn-W mineralization occurs as greisen zones and veins that crosscut the metasandstone with a NNW-SSE strike and a dip of 75° to 90° (Fig. 5F). Vein thicknesses range from 3 to 35 cm and some veins exhibit a sheeted internal structure composed of several incremental growth stages. The veins contain cassiterite and wolframite as the main ore minerals, which are associated with chalcopyrite, pyrite, sphalerite, molybdenite, galena, bismuthinite, fluorite, muscovite, calcite, and topaz (Aung Zaw Myint et al., 2017a). The ore minerals are strongly associated with muscovite patches in the greisen veins (Fig. 5G), which contain between 0.35 and 2.42 wt.% Sn (Kyaw Zay Ya, 2013). Common gangue minerals in the veins are quartz, K-feldspar, fluorite, muscovite, and calcite with trace amounts of topaz. Euhedral crystals of cassiterite occur as the major ore mineral and coexist with sulfide minerals and muscovite (Aung Zaw Myint, 2015; Aung Zaw Myint et al., 2017a). LA-ICP-MS U–Pb dating of cassiterite from a greisen vein at Bawapin yielded an age of 60.7 ± 2.5 Ma (2σ, n=29, MSWD=3.0), which matches well with that of the host granites in the region (Li et al., 2018b).

The mineralized quartz veins at Kalonta trend NS and NNW-SSE and crosscut the sedimentary rocks and granite. The host granite is partly greisenized and contains wolframite and lesser cassiterite as the main ore minerals (Fig. 5H). The W-Sn ore minerals are mostly associated with molybdenite, pyrite, galena, fluorite, and specularite. The veins from the northern part of the deposit are present in partially to pervasively greisenized granite, whereas those in the south are hosted by metasediments. Greisenization occurs both along the vein margins and more pervasively in the upper part of the granite cupolas. The greisen zones are mainly composed of quartz and muscovite, with subordinate amounts of fluorite, cassiterite, and wolframite. Silicification is the predominant alteration in the mineralized zone and associated with greisenization. In places, kaolinization related to argillic alteration is present as well, and characterized by the mineral association of kaolinite with other clay minerals such as illite and smectite (Aung Zaw Myint, 2019). The LA-ICP-MS U–Pb dating of cassiterite from mineralized quartz veins at Kalonta yielded an age of 64.6 ± 3.9 Ma (2σ, n=37, MSWD=3.5) (Li et al., 2018b).

The Kanbauk area, located in the northernmost part of the Dawei Sn-W region, is well-known for its W-Sn veins, but the main ore zone also contains a Sn-W-F skarn system. The deposit is developed at an apical zone of an elongate aplogranite stock that intrudes the mudstones of the Mergui Group and limestones of likely Permian age, resulting in the formation of an exoskarn zone. The skarn zone occurs as an irregularly-shaped body between the metasedimentary rocks and the marble, and is composed of diopside, garnet, wollastonite, hornblende, calcite, chlorite, cassiterite, magnetite, fluorite, scheelite, vesuvianite, pyrite, pyrrhotite, chalcopyrite, sphalerite, arsenopyrite, bismuthinite, and galena (Aung Zaw Myint, 2019).

3. Analytical methods

3.1 Mineralogical studies

Minerals and textural relationships were examined by a transmitted and reflected light optical microscope. The SEM-EDS determination of some sulfide minerals and the quantitative EPMA analysis of wolframite was performed with a JEOL JXA-8900R electron probe microanalyzer (EPMA), at the Institute of Applied Mineralogy and Economic Geology, at RWTH Aachen University. Quantitative analyses for W, Sn, Fe, Mn, Nb, Ta, and Ca were performed using an acceleration potential of 20 kV with a beam current of 25 nA. The intensity of X-Ray was accumulated for 10s and 5s for peaks and backgrounds, respectively.

3.2 Re-Os geochronology

Thirteen rhenium-osmium (Re-Os) analyses of molybdenite were carried out in order to determine the timing of greisen-associated mineralization at Pyiyadana (n = 2), Shwechaung (n = 5), Tagun Taung (n = 5), and Wagone (n = 1). Pyiyadana samples were collected from the tin-rich greisen patches, whereas Shwechaung, Tagun Taung, and Wagone samples were from tungsten and molybdenum-rich quartz veins. All molybdenite-bearing samples were obtained from undeformed vein sections thereby limiting the potential for any ^{187}Re-^{187}Os decoupling (Stein et al., 2003). Molybdenite Re-Os analysis (with the exception of the Wagone deposit sample) was conducted at the State Key Laboratory of Isotope Geochemistry, Guangzhou Institute of Geochemistry (GIG), Chinese Academy of Sciences. The single sample from Wagone was analyzed at the Durham Geochemistry Center (DGC), Durham University, United Kingdom.

Mineral separates were obtained using traditional isolation methods (e.g., crushing, magnetic, and/or heavy liquid separation) at the noted laboratories. At GIG, molybdenite flakes (grain size, 3-8 mm) were crushed using an agate pestle and then, screened by a 100 mesh (149 µm). Molybdenite grains were then handpicked under a binocular microscope to remove impurities. Similarly, at DGC a 200 to 70 mesh (74-210 µm) pure fraction of molybdenite

(~0.5g) was obtained for the Wagone sample. The Carius tube method was used for the dissolution of the molybdenite and equilibration of the samples with a Re and Os tracer solution. Molybdenite was dissolved and equilibrated with ^{185}Re and ^{190}Os spike solutions at the Guangzhou Institute of Geochemistry (Li et al., 2014 , 2015), and with a mixed ^{185}Re + Os (normal isotopic composition) spike at Durham University (Selby and Creaser, 2001). About 0.05–0.2 g of each molybdenite separate was digested and equilibrated with a tracer solution in reverse aqua regia (6 ml concentrated HNO_3 + 2 ml concentrated HCl) for 24 h at 240 °C in a sealed Carius tube. Osmium was extracted by solvent extraction into CCl_4 (GIG) or $CHCl_3$ (DGC) and back-extracted into concentrated HBr. The osmium fraction was further purified using subsequent microdistillation. The Re fraction was separated and purified using anion column chromatography (GIG), and by NaOH-C_3H_6O solvent extraction and anion chromatography (DGC). At GIG, osmium was loaded onto Pt filaments and measured as OsO_3 − ions by negative-thermal ionization mass spectrometry (N-TIMS) using the electron multiplier mode on a Thermo-Scientific Triton.

Repeated analyses of the Os standard solution (Merck Chemical AA standard solution) yield a mean $^{187}Os/^{188}Os$ value of 0.12050 ± 0.00030 (2 SD, n = 5) for the period of analysis. These values are in good agreement with a value of 0.12022 ± 0.00020 (2 SD, n = 14) measured on the same mass spectrometer in Faraday cup mode (Li et al., 2010). The rhenium mass fraction was analyzed by inductively coupled plasma mass spectrometry (Thermo Elemental X2 Series) at GIG. A conventional low volume quartz impact bead spray chamber with a Peltier cooled (3 °C) and a 0.4 ml min−1 borosilicate nebulizer (MicroMist GE) were used in the determinations. Ion lens settings, nebulizer gas flow rate and torch position were optimized daily using a 10 ng ml^{-1} tuning In–Ce mixture standard solution in order to obtain the high instrumental sensitivity and low oxide production levels. A peristaltic pump was not used, as free aspiration of the nebulizer provided better signal stability. Total procedural blanks were

0.82 ± 0.44 pg (1σ, n = 2) with an $^{187}Os/^{188}Os$ ratio of 0.67 ± 0.55 (1σ, n = 2) on average for Os and 4.8 ± 0.2 pg (1σ, n = 2) for Re. All data were corrected for the procedural blank for each analytical batch, but blank contributions were generally insignificant. At Durham, both rhenium and osmium isotope measurements were conducted using negative ionization mass spectrometry on a Thermo-Scientific Triton mass spectrometer. A full analytical protocol blank run along with the molybdenite analysis yielded 2.5 pg Re and 0.7 pg Os, with the latter possessing a $^{187}Os/^{188}Os$ isotopic composition of 0.21 ± 0.10. Details of the data treatment, standards and reference materials are given in Li et al. (2017). The analysis of the Wagone sample was conducted during the same time period as that of the Li et al. (2017) study at DGC. Molybdenite Re-Os model ages are calculated using a ^{187}Re decay constant of $1.666 \times 10^{-11}\ y^{-1}$ with an uncertainty of 0.31% (Smoliar et al., 1996; Selby et al., 2007). Isoplot v.4.15 (Ludwig, 2003) was used to calculate the ^{187}Re-^{187}Os isochron ages.

4. Results

4.1 Mineralogy and paragenesis

In the Padatgyaung W-Sn(-Mo) region, the tin-rich greisen mineralization is present as irregular patches, comprising mainly cassiterite, molybdenite, and minor wolframite, and as veins and narrow zones adjacent to veins, containing cassiterite, wolframite, and fluorite with the sulfide minerals arsenopyrite, molybdenite, pyrite, sphalerite, chalcopyrite, and galena. Scheelite occurs as a rare minor mineral in the greisen veins, and wolframite rarely occurs in the patches but forms a major mineral in the veins. These two sub-types (different mineralization styles) may be formed synchronously (Fig. 6). Some of the veins are not Sn-mineralized but are tungsten-rich quartz veins that carry a considerable amount of wolframite and molybdenite with minor to rare amounts of cassiterite, pyrite, and sphalerite.

Cassiterite occurs as weakly zoned to un-zoned crystals mainly enclosed in and overgrown by mica and quartz (Fig. 7A). Wolframite mostly occurs as clusters of bladed or prismatic crystals that are replaced by later-formed sulfides (Fig. 7B, C). Arsenopyrite and pyrite are generally early-formed sulfides and they are replaced and veined by later-formed sulfides such as chalcopyrite, sphalerite, and galena (Fig. 7D, E). Wolframite, which is the main tungsten-bearing mineral in the deposits of the region, has a Fe/(Fe+Mn) values ranging from 0.14 to 0.64 (Table 1). Fe-rich wolframite (ferberite) is common in the W-rich quartz veins, whereas the wolframite in Sn-rich greisen is generally hubneritic. Arsenopyrite contains As, Fe, and S ranging from (41.53 to 45.31 wt.% As), (34.16 to 35.98 wt.% Fe), and (20.53 to 22.64 wt.% S), respectively. Sphalerite is Fe-poor, as shown by energy-dispersive X-ray spectrometry (EDS).

The mineral paragenetic sequence of the Sn-W-(Mo) mineralization in the Dawei region is variable for each type of deposit. Generally, oxide ore minerals (the major Sn-W minerals cassiterite and wolframite) are deposited at the onset of vein formation. Cassiterite is generally zoned and pleochroic, and mainly associated with quartz and muscovite (i.e., greisen) (Fig. 7F, G, H). Wolframite coexists with quartz and muscovite (Fig. 7I, J) as well as with sulfide minerals (Fig. 7K). Common sulfide minerals are predominant in the tin-rich vein systems of Hermyingyi, Bawapin (Fig. 7L), and Kalonta. By contrast, molybdenite is prevalent in the tungsten-rich veins (e.g., Putletto, Wagone) except in some veins of the Hermyingyi deposit. It is important to note that magnetite is a common minor oxide mineral in the Wagone, Kalonta, and Kanbauk deposits, and is closely associated with Sn-W minerals.

The wolframite composition in the Hermyingyi and Wagone deposits is generally hubneritic while that in Kanbauk is mostly ferbritic (Table 1). Sphalerite has a moderate amount of Fe in the range of 3 to 5 wt.% at Bawapin and 5 to 7 wt.% at Hermyingyi.

4.2 Re-Os geochronology

The Re-Os abundances and model ages of quartz vein- and greisen-hosted molybdenite are listed in Table (2). The Padatgyaung molybdenites contain ^{187}Re and ^{187}Os abundances of 0.054 to 5.952 ppm, and of 0.018 to 5.984 ppb, respectively, with the Re-Os data yielding ages of 58.7 to 68.8 Ma (n=13). For Pyiyadana the two analyses yield Re-Os ages of 67.7 ± 5.1 Ma and 68.8 ± 3.2 Ma, which yield a weighted average of 68.5 ± 2.7 Ma (MSWD=0.14) (Fig. 8A). The Re-Os model ages of the Shwechaung molybdenite are not uniform and range from 58.73 ± 0.7 Ma to 64.4 ± 0.7 Ma. Three samples yield similar Re-Os ages (Table 2; Fig. 8B), which yield a weighted average of 64.23 ± 0.49 Ma (MSWD=0.49). Five Re-Os ages (60.5 ± 2.7 Ma to 61.5 ± 2.7 Ma) of molybdenites from Tagun Taung constrain a weighted average age of 60.54 ± 0.45 Ma (MSWD=1.3) (Fig. 8C) and a Re-Os isochron age of 60.4 ± 1.2 Ma (MSWD=3.8; initial ^{187}Os= 0.001 ± 0.064 ppb) (Fig. 8D). The molybdenite sample from the Wagone deposit possesses 0.017 ppm ^{187}Re and 18.3 ppt ^{187}Os. The Re-Os data yield a Re-Os model age of 64.47 ± 3.67 Ma.

5. Discussion

5.1 Timing of Sn-W (-Mo) mineralization and related granitic magmatism

The Re-Os molybdenite geochronology provides new constraints for the timing of mineralization at Padatgyaung. The weighted average Re-Os age of molybdenite from Pyiyadana of 68.5 ± 2.7 Ma constrains the timing of the tin-rich greisenization stage at Padatgyaung, which is identical within uncertainty with the Re-Os isochron age obtained for Hermyingyi (68.4 ± 2.5 Ma; Jiang et al. 2019). This mineralization age is older than the Re-Os isochron age of vein molybdenite from Tagun Taung (60.5 ± 0.7 Ma), as well as the Re-Os model ages (58.7 ± 0.7 Ma and 61.6 ± 0.7 Ma) and the weighted average Re-Os model age (64.2 ± 0.5 Ma) of molybdenite from the Shwechaung quartz veins. Therefore, the formation of the W-Mo veins occurred clearly later than tin greisen mineralization at Padatgyaung. The relatively younger age (58.7 Ma) of the molybdenite sample from Shwechaung is considered to have been affected by Re-Os decoupling. This was probably caused by the analysis of only small sample aliquot of the relatively coarse-grained (8 mm grain size) molybdenite in sample SC-4 (Stein et al., 2003; Selby and Creaser, 2004; Zhai et al., 2019).

Based on rather poorly constrained K-Ar age data, it was previously concluded that the Padatgyaung granite was emplaced at around 55 to 57 Ma (Brook and Snelling, 1976). These K-Ar ages are nominally younger than the new Re-Os molybdenite ages of this study, which provide robust time constraints on the vein formation. Therefore, the younger K-Ar ages most likely reflect hydrothermal overprinting and partial resetting of the K-Ar system in the host granites. An alternative interpretation of the younger K-Ar ages would be that part of the granite pluton hosting the Sn-W mineralization was emplaced during a later magmatic phase that occurred after the Cretaceous to Paleocene mineralization. The robustness of the K-Ar data would need to be tested by modern U-Pb or Ar-Ar dating techniques. Given that it has been shown that the Re-Os systematics in molybdenite is generally not affected by post-ore hydrothermal activity (Stein et al., 2001), the magmatic age of the Padatgyaung Sn-W mineralization is taken to be the age of greisenization (around 70 Ma). This magmatic event probably occurred synchronously with the emplacement of the 71 Ma old Nattaung granite that is located about 100 km NW of Padatgyaung (Mitchell et al., 2012).

On the other hand, the newly obtained Re-Os model age of 64.5 ± 3.7 Ma from the Wagone quartz vein system, in conjunction with previously determined cassiterite U-Pb ages (60 to 65 Ma) and the Re-Os molybdenite ages (68 Ma) from Dawei, do strongly support a major Late Cretaceous to Paleocene ore-forming hydrothermal system in the region. All the modern mineralization ages obtained by Re-Os and U-Pb methods are in good agreement with the U-Pb zircon ages of tin granite emplacement at Hermyingyi (61.4 ± 0.6 Ma and 70.4 ± 0.4 Ma) and Wagone (61.4 ± 0.5 Ma and 60.7 ± 3.5 Ma).

The molybdenite samples from the Padatgyaung Sn-W mineralization contain rather variable Re contents between 79 and 7600 ppb. Combining these data with Re concentration data from previous studies of molybdenite from Hermyingyi (Jiang et al., 2019), the Re contents in molybdenite from the Dawei region are generally below 1 ppm (i.e., 23 ppb to 300 ppb), and therefore lower than those from Padatgyaung. Together, the data show that the Re contents are low (<8ppm) in both ore systems, which is probably compatible with a crustal source for the Sn-W mineralization in the region (Mao et al., 1999; Stein, 2006). In general, molybdenite from Sn-W (-Mo) deposits associated with magmas derived mainly from the continental crust (e.g., Nanling region, China) possess very low rhenium abundances (< 10 ppm; Peng et al., 2006; Feng et al., 2011). In contrast, molybdenite from the W-Mo deposits, that are related to a magma possessing a minor mantle component (e.g., Jiangnan Tungsten belt, China), is characterized by slightly more elevated rhenium abundances (6.4–19 ppm, Song et al., 2012; 7.8–51 ppm, Li et al., 2015).

In addition, Early Cretaceous to Paleocene granites from the Tengchong terrane may have been derived from the partial melting of ancient crustal rocks with or without mixing with metaigneous rocks (Zhao et al., 2017; Fang et al., 2018). The Cretaceous tin granite (70 Ma) in Hermyingyi deposit has low εNd (t) (−11.3 to −10.6) and εHf(t) (−12.4 to −10.0) values, which indicate a crustal-derived melt source and support the interpretation of the Re concentration data that fertile granites were generated from partial melting of the old crustal blocks with no or little mantle contribution (Jiang et al., 2017). Moreover, the U-Pb age of 61 Ma for the Wagone and Hermyingyi granites has been interpreted in terms of a crustal-derived origin where the granitic melts were produced by partial melting of a felsic clay-rich source in a back-arc extensional setting (Li et al., 2018a). By interpretation on the geochemical and Sr–Nd–Hf isotopic characteristics, the magmas may have ascended relatively slowly in the crust and experienced some degree of fractional crystallization and assimilation and contamination by upper crustal material of Sibumsu, contributing to the extensive Sn–W mineralization in the Dawei area (Li et al., 2019). Meanwhile, magma with low degree of fractional crystallization and relatively high mantle components produced the formation of I-type granites (Li et al., 2019). The low concentrations of rhenium in molybdenite may also support the hypothesis that the ore metals that were deposited from magmatic-hydrothermal systems also had a crustal source.

5.2 Sn-W metallogeny in Myanmar and link to Western Yunnan in China

The available geochronological and geochemical data for the Sn-W deposits and host granites in the Sibumasu and Tengchong terranes suggest a possible genetic link between Sn-W mineralization in an extensive Sn-W mineral belt extending from southern Myanmar to western Yunnan (Mitchell, 2018; Aung Zaw Myint et al., 2018; Li et al., 2018b). The geochronological data constrain the granite-related Sn-W (-Mo) mineralization in the Western Granite Province to the Cretaceous to Eocene (Table 3; Fig. 9). The Sn-W mineralization in the Western Granite Province emerges at Tieyaoshan, Dabinga, and Mawpalaw Taung at 120-110 Ma (Mi Paik, 2017; Li et al., 2018b). The tin-rich (with no W and Mo) quartz and pegmatite veins with greisen systems are developed in biotite granites at Tieyaoshan and Mawpalaw Taung, while Mo (-W) bearing quartz veins are confined to the biotite granite of Dabinga. This Early Cretaceous magmatic event is probably related to the long-lasting subduction of the Meso-Tethyan plate that resulted in the collision and crustal thickening processes which were able to trigger partial melting of old crustal material with the minor addition of mantle material (Xu et al., 2012; Li et al., 2018b). The Early Cretaceous hydrothermal event resulted in two separate systems of Sn-rich (in both Sibumasu and Tengchong terranes) and W-Mo rich (in the Tengchong terrane only) ore systems forming as medium- to small-sized deposits.

After the Early Cretaceous collision in West Myanmar and the Sibumasu-Tengchong area (Metcalfe, 2013; Liu et al., 2016), low-angle subduction of the Neo-Tethyan oceanic lithosphere caused the development of an Andean-type magmatic arc with Late Cretaceous-Paleocene (100–50 Ma) felsic magmatism in the Western Granite Province (Mitchell et al., 2012; Gardiner et al., 2016, 2018; Jiang et al., 2017; Zhao et al., 2017; Fang et al., 2018) (Fig. 10).

Roll-back of the Neo-Tethyan oceanic slab is then proposed to have produced crustal derived melts that underwent high degrees of fractional crystallization and subsequent fluid exsolution (Jiang et al., 2017; Li et al., 2018b; Mao et al., 2020), which finally formed most of the Sn-W (-Mo) deposits in the Western Granite Province. Many large-scale deposits (e.g., Xiaolonghe, Hermyingyi, Kanbauk, and Myinmahti) as well as medium to small-scale deposits (e.g., Pilok, Tagu (Kuntabin), Sn-W-Mo deposits of Padatgyaung and Dawei regions) are characterized by an assemblage of quartz and pegmatite veins, greisens, and skarn mineralizations which represent the Late Cretaceous to Paleocene event. The significant difference between the greisen-type ore mineralization in the western part of Sibumasu and those in the Tengchong terrane is the lack of tungsten and molybdenum in the latter. Conversely, a significant number of vein systems in the western part of the Sibumasu terrane lack tin (e.g., Shwechaung, some veins of Wagone).

During the collision between India and Asia at around 50 Ma in the early Eocene, some tin granites with large to medium-scale Sn-W deposits (e.g., Lailishan, Yadanabon) have formed in the Western Granite Province, but the number of tin granites and related ore deposits that occurred during this period are much smaller compared to the major Late Cretaceous-Paleocene event. Partial melting of old crustal material and protracted fractional crystallization are crucial factors for producing the chemically evolved and metal enriched magma that was emplaced into the shallow crust as fertile tin granites (Gardiner et al., 2016, 2018; Aung Zaw Myint et al., 2018; Li et al., 2018b).

Emplacement of late Eocene granites (42 Ma) at Mawchi, the youngest tin-tungsten mineralized granite in the Western Granite Province, is probably the product of a tectonic environment that was different from the setting that caused the formation of the older tin granites. The Eocene granites most likely represent late collisional (Gardiner et al., 2016, 2018) or post-collisional granites (Aung Zaw Myint et al., 2017b), which are probably originated from lithospheric thinning in response to the regional Late Eocene-Early Miocene extension (Mitchell et al., 2012; Morley, 2014). A geodynamic model of the Neo-Tethyan oceanic slab tear and break-off during the late- or post-collisional event is also proposed for the origin and emplacement of Eocene–Oligocene (45–30 Ma) mafic-felsic magmas and formation of related ore deposits in this Province (Li et al., 2018b).

Generally, the mineral deposits in the Tengchong terrane lack W-Mo minerals except few small veins at Dapinga, and this first-order feature is best interpreted to reflect the compositional differences between the corresponding old crustal sources of the Sibumasu and Tengchong terranes. Low contents of Re in hydrothermal molybdenite samples (2.9 to 8.3 ppm in Dabinga, 0.02 to 0.3 ppm in Dawei, 0.1 to 9.5 ppm in Padatgyaung and 1.4 ppm in Mawchi) also support that the ore metals are crustal-derived. Geochronological evidence for two or more episodes of mineralization within the same granite pluton (e.g., Dapingba, one event at 120–114 Ma and then a later one at ∼108 Ma; Hermyingyi, one event at 70 Ma and then at a later one at ∼60 Ma) suggests that the plutons were built up by multiple or successive magmatic stages which are linked with separate mineralization events in the Western Granite Province. In addition, the formation of tin greisens generally occurred earlier than the formation of vein type mineralization in greisen-rich Sn-W ore systems (e.g., Xiaolonghe, Lailishan, probably in Padatgyaung).

6. Conclusions

(1) Combining and integrating the new Re-Os geochronological data for molybdenite from two Sn-W regions with available Re-Os data for molybdenite and U-Pb data for host granites demonstrates that magmatic-hydrothermal activity and formation of ore deposits occurred as several discrete events in the Western Granite Province of SE Asia.

(2) Greisen formation initiated around 68 Ma and subsequent hydrothermal vein mineralization was formed during 65-61 Ma at Padatgyaung, characterized by the Re-OS ages of hydrothermal molybdenite. The Re-Os model age of the quartz-molybdenite veins (63 Ma) from Wagone, combined with previous U-Pb (60.7±2.5 Ma to 64.6±3.9 Ma) and Re-Os (68.4±2.5 Ma) data, confirms a Late Cretaceous-Paleocene ore forming episode in the Dawei Sn-W region.

(3) Our new geochronological data, in conjunction with geological data, mineralogy and ore paragenetic stages and existing age data for the Sn-W mineralization and granite emplacement, support extensive granite-associated Sn-W(-Mo) mineralization events in the Western Granite Province during ca. 75 Ma and 60 Ma probably associated with the collision regime developed at that time.

(4) Roll-back of the Neo-Tethyan oceanic slab was responsible for the emplacement of crustally derived melts that underwent high degrees of fractional crystallization and subsequent post-magmatic ore fluid produced the Sn-W (-Mo) deposits in the Western Granite Province.

(5) Metal constituents in the Sn-W- (Mo) deposits were considered to have derived from the crustal blocks, as indicated by the quite low Re content (< 10 ppm) in hydrothermal molybdenite samples.

Acknowledgements

The Alexander von Humboldt Foundation is acknowledged for providing a Georg Forster fellowship to the first author. Roman Klinghardt assisted with the EPMA analysis of wolframite. The authors are deeply indebted to Professor Khin Zaw, CODES, University of Tasmania for his editorial handling, valuable advice, and constructive suggestions. We would like to thank two anonymous reviewers for their critical and constructive reviews.

References

Aung Zaw Myint, 2015. Granite-related Sn-W-REE mineralization in Mawchi and Dawei areas, Myanmar. PhD Dissertation, Kyushu University, 127p.

Aung Zaw Myint, 2019. Geological studies of Sn-W deposits in Dawei Area, Tanintharyi Region. Unpublished research report, Department of Higher Education, Ministry of Education, Myanmar, 27p.

Aung Zaw Myint, Suzaki, R., Yonezu, K., Watanabe, K., Kyaw Zay Ya, 2014. Geology of Dawei Sn-W District, Myanmar. Proceedings of international symposium on Earth science and technology 2014, Fukuoka, Japan, 244−246.

Aung Zaw Myint, Yonezu, K., Watanabe, K., 2017a. Granite-related Sn-W mineralization in Dawei, southern Myanmar. Proceedings of 7th Asia Africa Mineral Resources Conference, Yangon, Myanmar, 115−117.

Aung Zaw Myint, Khin Zaw, Ye Myint Swe, Yonezu, K., Cai, Y., Manaka, T., Watanabe, K., 2017b. Geochemistry and geochronology of granites hosting the Mawchi Sn-W deposit, Myanmar: implications for tectonic setting and granite emplacement, In: Barber AJ, Crow MJ, Khin Zaw (Eds.), Myanmar: Geology, Resources and Tectonics, Geological Society, London, Memoirs 48, 385−400.

Aung Zaw Myint, Yonezu, K., Boyce, A., Selby, D., Scherstén, A., Tindell, T., Watanabe, K., Ye Myint Swe, 2018. Stable isotope and geochronological study of the Mawchi Sn-W deposit, Myanmar: implications for timing of mineralization and ore genesis. Ore Geology Reviews 95, 663−679.

Aung Zaw Myint, Yadana Tun, Chit Ko Win, Maung Maung Oo, Min Myo Ko Ko, 2019. Mineralogical and geochemical constraints on the genesis of granite-related W -Sn -Mo mineralization in Padatgyaung-Myinmahti area, central Myanmar. Journal of Myanmar Arts and Sciences Academy, 17, 1−18.

Barley, M.E., Pickard, A.L., Khin Zaw, Rak, P., Doyle, M.G., 2003. Jurassic to Miocene magmatism and metamorphism in the Mogok metamorphic belt and the India-Eurasia collision in Myanmar. Tectonics 22, 10−19.

Bateson, J.H., Mitchell, A.H.G., Clarke, D.A., 1972. Geological and geochemical reconnaissance of the Seikphudaung- Padatgyaung area of Central Burma. Institute of Geol Sci, London, Overseas Division Report 25, 54p.

Bender, F.K., 1983. Geology of Burma. Gebruder Borntraeger Verlagsbuchhandlung, Science Publishers, 293p.

Brook, M., Snelling, N.J., 1976. K/Ar and Rb/Sr age determinations on rocks and minerals from Burma. London, Institute of Geological Science Isotope Geology Unit Rep 76/12.

Brown, J.C., Heron, A.M., 1923. The geology and ore deposits of Tavoy District. Memoir of Geological Survey of India, 44, 167-354.

Cao, H.W., Zhang, Y.H., Tang, L., Hollis, S.P., Zhang, S.T., Pei, Q.M., Yang, C., Zhu, X.S., 2019. Geochemistry, zircon U–Pb geochronology and Hf isotopes of Jurassic-Cretaceous granites in the Tengchong terrane, SW China: implications for the Mesozoic tectono-magmatic evolution of the Eastern Tethyan Tectonic Domain. International Geological Reviews 61, 257−279.

Charusiri, P., 1989. Lithophile metallogenetic epochs of Thailand: a geological and geochronological investigation. Unpubl PhD Thesis, Queen University, Kingston, Canada, 809p.

Charusiri, P., Clark, A.H., Farrar, E., Archibald, D., Charusiri, B., 1993. Granite belts in Thailand: evidence from the 40 Ar/39 Ar geochronological and geological syntheses. Journal of Southeast Asian Earth Sciences 8, 127–136.

Chen, X.C., Hu, R.Z., Bi, X.W., Li, H.M., Lan, J.B., Zhao, C.H., Zhu, J.J., 2014. Cassiterite LA-MC-ICP-MS U/Pb and muscovite 40Ar/39Ar dating of tin deposits in the Tengchong-Lianghe tin district, NW Yunnan, China. Mineralium Deposita 49, 843−860.

Chen, X.C., Hu, R.Z., Bi, X.W., Zhong, H., Lan, J.B., Zhao, C.H., Zhu, J.J., 2015. Petrogenesis of metaluminous A-type granitoids in the Tengchong–Lianghe tin belt of southwestern China: evidence from zircon U–Pb ages and Hf–O isotopes, and whole-rock Sr–Nd isotopes. Lithos 99, 57−71.

Clegg, E.L.G., 1944. Notes on tin and wolfram in Burma and India. Records of Geological Survey of India 76, 168p.

Cobbing, E.J., Mallick, D.I.J., Pitfield, P.E.J., Teoh, L.H., 1986. The granites of the Southeast Asian tin belt. Journal of Geological Society 143, 537−550.

Cobbing, E.J., Pitfield, P.E.J., Darbyshire, D.P.F., Mallick, D.I.J., 1992. The granites of the South-East Asian tin belt. Overseas Memoir 10, British Geological Survey.

Cong, F., Li, W.C., Wu, F.Y., Huang, L., Huang, X.M., Sun, J., Liu, X.C., Hu, F.Y., Hu, S.X., Wu, G.H., 2020. Mesozoic crustal growth in Mainland Southeast Asia: Zircon U-Pb and Hf isotopic evidence from the Late Cretaceous Luyingtang granitic pluton in the northernmost SE Asian granite Province, SW China. Journal of Asian Earth Sciences 190, 104151.

Crow, M.J., Khin Zaw, 2017. Appendix Geochronology in Myanmar (1964–2017), In: Barber AJ, Crow MJ, Khin Zaw (Eds.), Myanmar: Geology, Resources and Tectonics, Geological Society, London, Memoirs 48, 713−759

Fang, Y., Zhang, Y.H., Zhang, S.T., Cao, H.W., Zou, H. and Dong, J.H., 2018. Early Cretaceous I-type granites in the Tengchong terrane: New constraints on the late Mesozoic tectonic evolution of southwestern China. *Geoscience Frontiers*, *9*(2), pp.459-470.

Feng, C.Y., Zeng, Z.L., Zhang, D.Q., Qu, W.J., Du, A.D., Li, D.X., She, H.Q., 2011. SHRIMP zircon U–Pb and molybdenite Re-Os isotopic dating of the tungsten deposits in the Tianmenshan–Hongtaoling W–Sn ore field, southern Jiangxi Province, China, and geological implications. Ore Geology Reviews 43, 8–25.

Gardiner, N.J., Robb, L.J., Morley, C.K., Searle, M.P., Cawood, P.A., Whitehouse, M.J., Kirkland, C.L., Roberts, N.M.W., Tin Aung Myint, 2016. The tectonic and metallogenic framework of Myanmar: A Tethyan mineral system. Ore Geology Reviews 79, 26−45.

Gardiner, N.J., Searle, M.P., Morley, C.K., Robb, L.J., Whitehouse, M.J., Roberts, N.M., Kirkland, C.L., Spencer, C.J., 2018. The crustal architecture of Myanmar imaged through zircon U-Pb, Lu-Hf and O isotopes: Tectonic and metallogenic implications. Gondwana Research 62, 27−60.

Harris, N.B.W., Pearce, J.A., Tindle, A.G., 1986. Geochemical characteristics of collision-zone magmatism. Geological Society Special Publication 19, 67–81.

Hobson, G.V., 1940. The development of the mineral deposit at Mawchi as determined by its geology and genesis. Transactions of the Mines, Geological and Metallurgical Institute of India 36, 35–78.

International Tin Research Institute (ITRI), 2016. Report on global tin sources and reserves. 20p.

Jiang, H., Jiang, S.Y., Li, W., Zhao, K., 2019. Timing and Source of the Hermyingyi W-Sn Deposit in Southern Myanmar, SE Asia: Evidence from Molybdenite Re-Os Age and Sulfur Isotopic Composition. Journal of Earth Science 30, 70−79.

Jiang, H., Li, W.Q., Jiang, S.Y., Wang, H., Wei, X.P., 2017. Geochronological, geochemical and Sr-Nd-Hf isotopic constraints on the petrogenesis of Late Cretaceous A-type granites from the Sibumasu Block, Southern Myanmar, SE Asia. Lithos 268, 32−47.

Kalsbeek, F., Jepsen, H.F., Nutman, A.P., 2001. From source migmatites to plutons: tracking the origin of c. 435 Ma S-type granites in the East Greenland Caledonian orogen. Lithos, 57, 1–24.

Khin Zaw, 1990. Geological, petrogical and geochemical characteristics of granitoid rocks in Burma: with special reference to the associated W-Sn mineralization and their tectonic setting. Journal of Asian Earth Sciences 4, 293−335.

Khin Zaw, 2017. Overview of Mineralization Styles and Tectonic—Metallogenic Setting in Myanmar. In: Barber, A.J., Khin Zaw, Crow, M.J. (Eds.), Myanmar: Geology, Resources and Tectonics, the Geological Society (London) Memoir, Vol. 48, the Geological Society of London, London, 531-556. https://doi.org/10.1144/M48.24.

Khin Zaw, Khin Myo Thet, 1983. A note on a fluid inclusion study of tin-tungsten mineralization at Mawchi Mine, Kayah State, Burma. Economic Geology, 78, 530–534.

Kyaw Thu Htun, Yonezu, K., Aung Zaw Myint, Tindell, T., Watanabe, K., 2019. Petrogenesis, ore mineralogy, and fluid inclusion studies of the Tagu Sn–W deposit, Myeik, southern Myanmar. Minerals, 9, 654.

Kyaw Zay Ya, 2013. Geology and Tin-Tungsten Mineralization of Bawabin Area, Dawei Township, Tanintharyi Region, Myanmar. MSc thesis, University of Yangon, Myanmar.

Lehmann, B., 2020. Formation of tin ore deposits: A reassessment. Lithos, 105756. https://doi.org/10.1016/j.lithos.2020.105756

Li, C.H., Jiang, Y.H., Xing, G.F., Guo, K.Y., Li, C., Yu, M.G., Zhao, P., Wang, Z., 2015. Two periods of skarn mineralization in the Baizhangyan W-Mo Deposit, Southern Anhui Province, Southeast China: evidence from zircon U-Pb and molybdenite Re-Os and sulfur isotope data. Resource Geology 65, 193–209.

Li, H., Aung Zaw Myint, Yonezu, K., Watanabe, K., Algeo, T.J., Wu, J.H., 2018a. Geochemistry and U–Pb geochronology of the Wagone and Hermyingyi A-type granites, southern Myanmar: Implications for tectonic setting, magma evolution and Sn–W mineralization. Ore Geology Reviews 95, 575−592.

Li, J., Liang, X.R., Xu, J.F., Suzuki, K., Dong, Y.H., 2010. Simplified technique for the measurements of Re-Os isotope by multicollector inductively coupled plasma mass spectrometry (MC-ICP-MS). Geochemical Journal 44, 73−80.

Li, J., Jiang, X.Y., Xu, J.F., Zhong, L.F., Wang, X.C., Wang, G.Q., Zhao, P.P., 2014. Determination of Platinum-Group Elements and Re-Os Isotopes using ID-ICP-MS and N-TIMS from a Single Digestion after Two-Stage Column Separation. Geostandards and Geoanalytical Research 38, 37−50.

Li, J., Zhao, P.P., Liu, J.G., Wang, X.C., Yang, Y., Wang, G.Q., Xu, J.F., 2015. Reassessment of hydrofluoric acid desilicification in the carius tube digestion technique for Re-Os isotopic determination in geological Samples. Geostandards and Geoanalytical Research 39, 17−30.

Li, J.X., Zhang, L.Y., Fan, W.M., Ding, L., Sun, Y.L., Peng, T.P., Li, G.M., Kyaing Sein, 2018b. Mesozoic-Cenozoic tectonic evolution and metallogeny in Myanmar: Evidence from zircon/cassiterite U–Pb and molybdenite Re–Os geochronology. Ore Geology Reviews 102, 829−845.

Li, J.X., Fan, W.M., Zhang, L.Y., Evans, N.J., Sun, Y.L., Ding, L., Guan, Q.Y., Peng, T.P., Cai, F.L., Kyaing Sein, 2019. Geochronology, geochemistry and Sr–Nd–Hf isotopic compositions of Late Cretaceous–Eocene granites in southern Myanmar: Petrogenetic, tectonic and metallogenic implications. Ore Geology Reviews 112, 103031.

Li, Y., Selby, D., Condon, D., Tapster, S., 2017. Cyclic magmatic-hydrothermal evolution in porphyry systems: high-precision U-Pb and Re-Os geochronology constraints on the Tibetan Qulong porphyry Cu-Mo deposit. Economic Geology 112, 1419–1440.

Liu, C.Z., Chung, S.L., Wu, F.Y., Zhang, C., Xu, Y., Wang, J.G., Chen, Y., Guo, S., 2016. Tethyan suturing in Southeast Asia: Zircon U-Pb and Hf-O isotopic constraints from Myanmar ophiolites. Geology 44, 311–314.

Ludwig, K.R., 2003. A geochronological toolkit for Microsoft Excel. Berkeley Geochronology Center Special Publication 4, 1–70.

Mao, J., Zhang, Z., Zhang, Z., Du, A., 1999. Re-Os isotopic dating of molybdenites in the Xiaoliugou W (Mo) deposit in the northern Qilian mountains and its geological significance. Geochimica et Cosmochimica Acta 63, 1815−1818.

Mao, W., Zhong, H., Yang, J., Tang, Y., Liu, L., Fu, Y., Zhang, X., Kyaing Sein, Soe Myint Aung, Li, J., Zhang, L., 2020. Combined Zircon, Molybdenite, and Cassiterite Geochronology and Cassiterite Geochemistry of the Kuntabin Tin-Tungsten Deposit in Myanmar. Economic Geology 115, 603−625.

Metcalfe, I., 2013. Gondwana dispersion and Asian accretion: Tectonic and palaeogeographic evolution of eastern Tethys. Journal of Asian Earth Sciences 66, 1−33.

Mi Paik, 2017. Geochemistry and geochronology of granitoid rocks in the Mawpalaw Taung area, Thanbyuzayat Township, southern Myanmar: their petrogenesis and tectonic setting. In: Barber A.J., Khin Zaw, Crow M.J., (Eds.), Myanmar: Geology, Resources and Tectonics, Geological Society, London, Memoirs 48, 401−412.

Mitchell, A.H.G., 1977. Tectonic settings for emplacement of Southeast Asian tin granites. Geological Society of Malaysia Bulletin 9, 123–140.

Mitchell, A.H.G., 2018. Geological belts, plate boundaries, and mineral deposits in Myanmar. Elsevier, Amsterdam, 509p.

Mitchell, A.H.G., Ausa, C., Deiparine, L., Tin Hlaing, Nyunt Htay, Aung Khine, 2004. The Modi Taung-Nankwe gold district, Slate Belt, Central Myanmar: mesothermal veins in a Mesozoic orogen. Journal of Asian Earth Sciences 23, 321−341.

Mitchell, A.H.G., Myint Thein Htay, Kyaw Min Htun, Myint Naing Win, Thura Oo, Tin Hlaing, 2007. Rock relationships in the Mogok metamorphic belt, Tatkon to Mandalay, central Myanmar. Journal of Asian Earth Sciences 29, 891−910.

Mitchell, A.H.G., Chung, S.L., Thura Oo, Lin, T.H., Hung, C.H., 2012. Zircon U–Pb ages in Myanmar: Magmatic–metamorphic events and the closure of a neo-Tethys ocean? Journal of Asian Earth Sciences 56, 1−23.

Morley, C.K., 2014. The widespread occurrence of low-angle normal faults in a rift setting: Review of examples from Thailand, and implications for their origin and evolution. Earth-Science Reviews 133, 18−42.

Nandar Oo, 1980. Mineralogical characters and associations of the Heinda Deposit, Tavoy. MSc thesis, Rangoon Arts and Sciences University, Rangoon, Myanmar.

Nilar Shwe, 1981. Mineralogical study of the tin-tungsten deposit of the Hermyingyi Mine, Tavoy. MSc Thesis, Rangoon Arts and Sciences University, Rangoon, Myanmar.

Peng, J.T., Zhou, M.F., Hu, R.Z., Shen, N.P., Yuan, S.D., Bi, X.W., Du, A.D., Qu, W.J., 2006. Precise molybdenite Re-Os and mica Ar-Ar dating of the Mesozoic Yaogangxian tungsten deposit, central Nanling district, South China. Mineralium Deposita 41, 661–669.

Searle, D.L., Haq, B.T., 1964. The Mogok belt of Burma and its relationship to the Himalayan orogeny. Proceedings of the 22nd International Geology Conference, Delhi11, 132−161.

Searle, M.P., Noble, S.R., Cottle, J.M., Waters, D.J., Mitchell, A.H.G., Tin Hlaing, Horstwood, M.S.A., 2007. Tectonic evolution of the Mogok metamorphic belt, Burma (Myanmar) constrained by U-Th-Pb dating of metamorphic and magmatic rocks. Tectonics, 26.

Selby, D., Creaser, R.A., 2001. Late and mid-Cretaceous mineralization in the northern Canadian Cordillera: Constraints from Re-Os molybdenite dates. Economic Geology 96, 1461−1467.

Selby, D., and Creaser, R.A., 2004, Macroscale NTIMS and microscale LA-MC-ICP-MS Re-Os isotopic analysis of molybdenite: Testing spatial restrictions for reliable Re-Os age determinations, and implications for the decoupling of Re and Os within molybdenite. Geochimica et Cosmochimica Acta 68, 3897-3908.

Selby, D., Creaser, R.A., Stein, H.J., Markey, R.J., Hannah, J.L., 2007. Assessment of the 187 Re decay constant by cross calibration of Re–Os molybdenite and U–Pb zircon chronometers in magmatic ore systems. Geochimica et Cosmochimica Acta 71, 1999-2013.

Smoliar, M.I., Walker, R.J., Morgan, J.W., 1996. Re-Os ages of group IIA, IIIA, IVA, and IVB iron meteorites. Science 271, 1099-1102.

Song, G.X., Qin, K.Z., Li, G., Liu, T., Li, J., Li, X., Chang, Z., 2012. Geochronologic and isotope geochemical constraints on magmatism and associated W-Mo mineralization of the Jitoushan W-Mo deposit, middle-lower Yangtze Valley. International Geological Reviews 54, 1532–1547.

Stein, H.J., 2006. Low-rhenium molybdenite by metamorphism in northern Sweden: recognition, genesis, and global implications. Lithos 87, 300–327.

Stein, H.J., Markey, R.J., Morgan, J.W., Hannah, J.L., Scherstén, A., 2001. The remarkable Re–Os chronometer in molybdenite: how and why it works. Terra Nova 13, 479–486.

Stein, H., Scherstén, A., Hannah, J., Markey, R., 2003, Subgrain-scale decoupling of Re and 187Os and assessment of laser ablation ICP-MS spot dating in molybdenite. Geochimica et Cosmochimica Acta, 67, 3673-3686.

Than Htun, Than Htay, Khin Zaw, 2017. Tin–tungsten deposits of Myanmar. In: Barber, A.J., Khin Zaw, Crow, M.J. (Eds.), Myanmar: Geology, Resources and Tectonics, Geological Society, London, Memoirs 48, 625–647, https://doi.org/10.1144/M48.28

Xu, Y.G., Yang, Q.J., Lan, J.B., Luo, Z.Y., Huang, X.L., Shi, Y.R., Xie, L.W., 2012. Temporal–spatial distribution and tectonic implications of the batholiths in the Gaoligong–Tengliang–Yingjiang area, western Yunnan: constraints from zircon U–Pb ages and Hf isotopes. Journal of Asian Earth Sciences 53, 151−175.

Ye Zaw, Aung Zaw Myint, 2018. Granite-Related Tungsten-Tin Mineralization in Putletto area, Dawei Sn-W District, Southern Myanmar. Proceedings of the second Myanmar National Conference on Earth Sciences (MNCES 2018), 861−872.

Zhai, D., Williams-Jones, A.E., Liu, J., Selby, D., Li, C., Huang, X.W., Qi, L., Guo, D., 2019. Evaluating the Use of the Molybdenite Re-Os Chronometer in Dating Gold Mineralization: Evidence from the Haigou Deposit, Northeastern China. Economic Geology 114, 897-915.

Zhao, S.W., Lai, S.C., Qin, J.F., Zhu, R.Z. and Wang, J.B., 2017. Geochemical and geochronological characteristics of late cretaceous to early Paleocene granitoids in the Tengchong Block, Southwestern China: implications for crustal anatexis and thickness variations along the eastern Neo-Tethys subduction zone. *Tectonophysics*, *694*, pp.87-100.

Figure captions

Fig. 1. (A) Simplified tectonic subdivision map of Myanmar and the adjacent countries showing major geological units (adapted from Gardiner et al., 2016, 2018). (B) Granitoid belts of Myanmar and the adjacent region showing the main occurrences of granites and their geochronological ages (Aung Zaw Myint et al., 2018; modified after Cobbing et al., 1992; Mitchell et al., 2007; Sone and Metcalfe, 2008). Published zircon U-Pb age data for granites are from Mitchell et al. (2012), Chen et al. (2015), Gardiner et al. (2016), Aung Zaw Myint et al. (2017), Crow and Khin Zaw (2017), Jiang et al. (2017), Li et al. (2018a, 2018b), Cao et al. (2019), and Mao et al. (2020).

Fig. 2. Geological map of the Padatgyaung W-Sn (-Mo) region (Aung Zaw Myint et al., 2019; modified after Bateson et al., 1972).

Fig. 3. Field photographs and representative hand specimen photographs of the Sn-W mineralization in the Padatgyaung region. (A) Hand specimens collected from the irregularly shaped greisen patches. (B) Small quartz veins crosscutting the host rock mudstone at Pyiyadana. (C) Greisen-bordered quartz vein at Bularmi. (D) Wolframite-bearing quartz veins from Tayokegone. (E) Molybdenite-quartz vein specimens from Shwe Chaung. (F) Wolframite bearing quartz vein from Myinmahti. (G) Weathered quartz veins at Yadanagadaytike. (H) Quartz vein of the Tagun Taung deposit bordered by syn-vein greisenization with muscovite alteration.

Fig. 4. Geological map of the Dawei Sn-W (-Mo) region (Aung Zaw Myint, 2019; modified after Clegg, 1944; Bender, 1983; Aung Zaw Myint, 2015).

Fig. 5. Field photographs and hand specimen photographs of Sn-W mineralization in Dawei region. (A) Quartz + wolframite vein at Putlatto. (B) Hermyingyi veins in biotite granite. (C) Sub-economic quartz vein cutting the biotite granite. (D) Cassiterite and magnetite present as reddish brown patches in weathered granite. (E) Platy or massive molybdenite

from W-Mo quartz vein of Wagone. (F) Greisen vein in the Mergui Group at Bawapin. (G) Close-up view showing the association of ore minerals with muscovite patches in greisen vein. (H) Greisenized quartz vein at Kalonta containing cassiterite and wolframite.

Fig. 6. Paragenetic sequence of W-Sn(-Mo) mineralization at Padatgyaung.

Fig. 7. Photomicrographs of ore mineral assemblages from the Padatgyaung and Dawei regions. (A) Weakly zoned cassiterite from Pyiyadana. (B) Wolframite crystals from Shwechaung. (C) Cluster of bladed wolframite crystals from Tagun Taung. (D) Pyrite (py) and arsenopyrite replaced by sphalerite (sp) and chalcopyrite (cp) in Pyiyadana. (E) Deformed galena replacing pyrite in the Shwechaung vein. (F) Quartz veinlet crosscutting the zoned cassiterite at Bawapin. (G) Small cassiterite crystals enclosed in the quartz specimen from Kalonta. (H) Cassiterite mineralization at Taungphila. (I) Small wolframite clusters in quartz vein from Wagone. (J) Quartz vein containing wolframite and quartz replaced by chalcopyrite from Hermyingyi. (K) Wolframite grains in the quartz vein from Kanbauk. (L) Bismuthinite crystal cut by a trail of minute pyrite grains in greisen vein from Bawapin.

Fig. 8. Re-Os weighted average model ages of (A) Pyiyadana, (B) Shwechaung, and (C) Tagun Taung. (D) Re-Os isochron plot of Tagun Taung.

Fig. 9. Reconstructed temporal evolution of Sn-W metallogenesis in the Western Granite Province. Data sources: *current study, [1]Chen et al., 2014, [2]Li et al., 2018b, [3]Paik, 2017, [4]Chen et al., 2015, [5]Charusiri, 1989, [6]Jiang et al., 2017, [7]Li et al., 2018a, [8]Jiang et al., 2019, [9]Gardiner et al., 2016, [10]Aung Zaw Myint et al., 2017, [11]Aung Zaw Myint et al. 2018, [12]Mao et al. 2020.

Fig. 10. Tectonic model for the Sn-W(-Mo) mineralization at Pdatgyaung and Dawei (after Gardiner et al., 2016).

Fig. 1

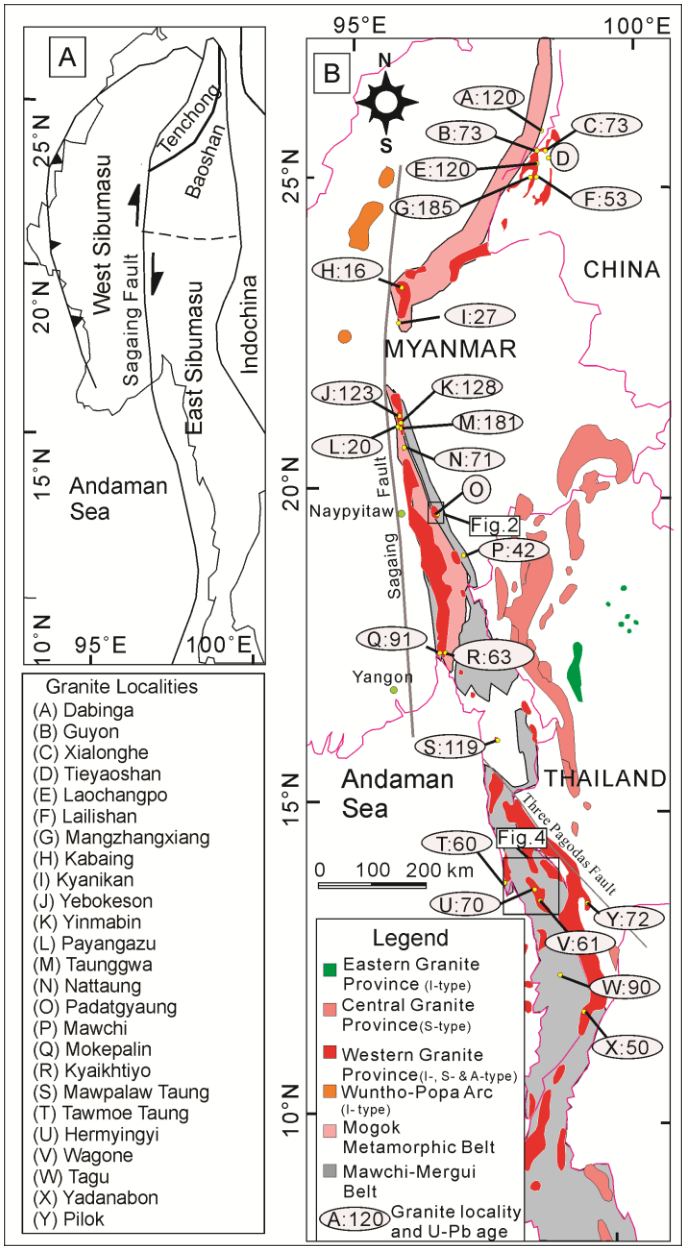

A
Tenchong
Baoshan
West Sibumasu
Sagaing Fault
East Sibumasu
Indochina
Andaman Sea
25°N
20°N
15°N
10°N
95°E
100°E
Granite Localities
(A) Dabinga
(B) Guyon
(C) Xialonghe
(D) Tieyaoshan
(E) Laochangpo
(F) Lailishan
(G) Mangzhangxiang
(H) Kabaing
(I) Kyanikan
(J) Yebokeson
(K) Yinmabin
(L) Payangazu
(M) Taunggwa
(N) Nattaung
(O) Padatgyaung
(P) Mawchi
(Q) Mokepalin
(R) Kyaikhtiyo
(S) Mawpalaw Taung
(T) Tawmoe Taung
(U) Hermyingyi
(V) Wagone
(W) Tagu
(X) Yadanabon
(Y) Pilok
B
N
S
95°E
100°E
A:120
B:73
C:73
D
E:120
F:53
G:185
H:16
I:27
J:123
K:128
M:181
L:20
N:71
O
Fig.2
P:42
Q:91
R:63
S:119
T:60
U:70
V:61
W:90
X:50
Y:72
Fig.4
CHINA
MYANMAR
THAILAND
Andaman Sea
Naypyitaw
Yangon
Sagaing Fault
Three Pagodas Fault
0 100 200 km
Legend
Eastern Granite Province (I-type)
Central Granite Province(S-type)
Western Granite Province(I-, S- & A-type)
Wuntho-Popa Arc (I- type)
Mogok Metamorphic Belt
Mawchi-Mergui Belt
A:120 Granite locality and U-Pb age

Fig. 2

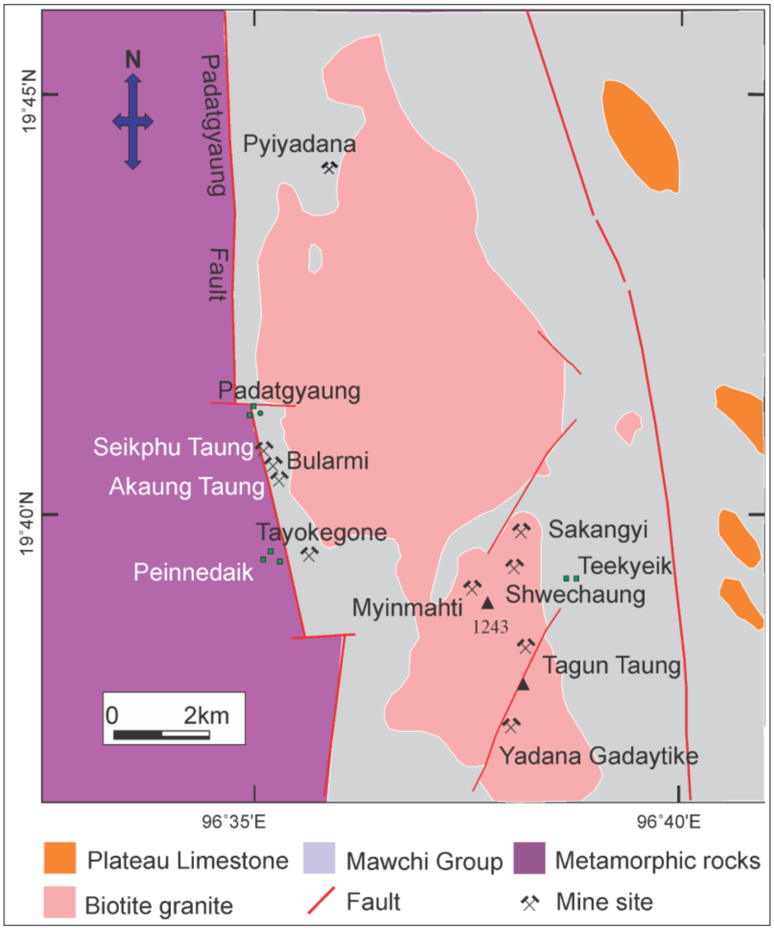
N
19°45'N
19°40'N
96°35'E
96°40'E
Padatgyaung Fault
Pyiyadana
Padatgyaung
Seikphu Taung
Bularmi
Akaung Taung
Tayokegone
Peinnedaik
Sakangyi
Teekyeik
Shwechaung
Myinmahti
1243
Tagun Taung
Yadana Gadaytike
0 2km
Plateau Limestone
Mawchi Group
Metamorphic rocks
Biotite granite
Fault
Mine site

Fig. 3

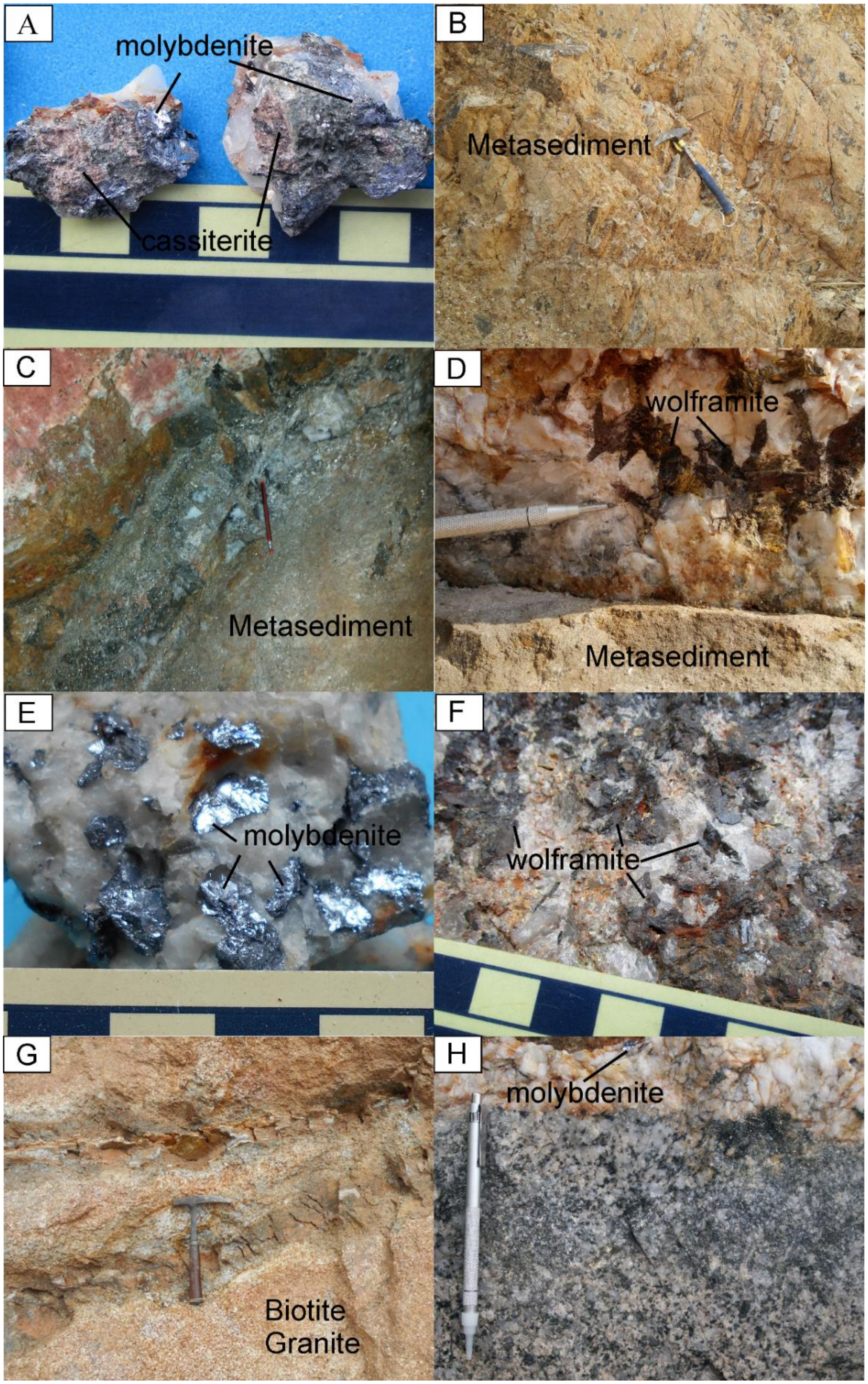
A
molybdenite
cassiterite
B
Metasediment
C
Metasediment
D
wolframite
Metasediment
E
molybdenite
F
wolframite
G
Biotite
Granite
H
molybdenite

Fig. 4

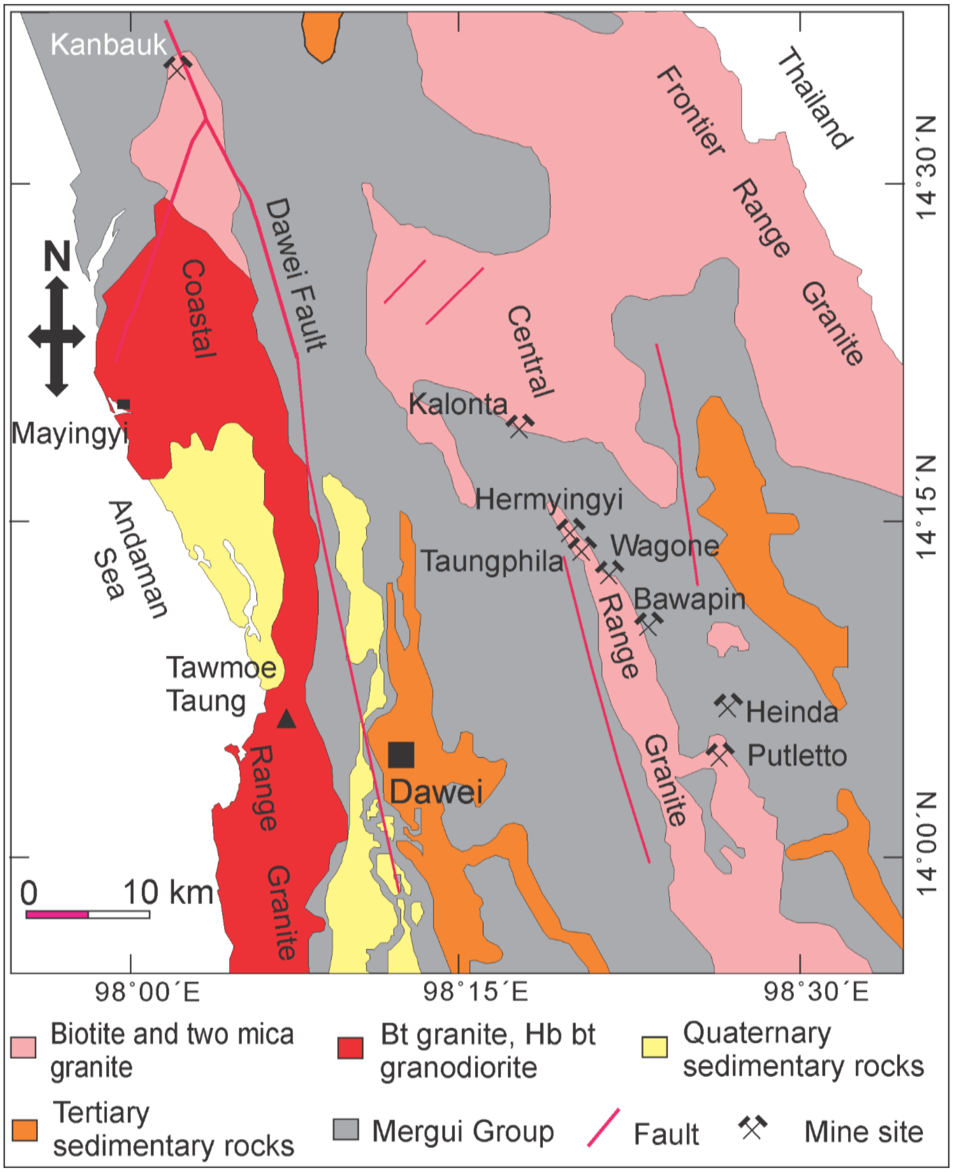

Kanbauk
Thailand
Frontier Range Granite
Dawei Fault
Coastal Range Granite
Central Range Granite
N
Kalonta
Mayingyi
Hermyingyi
Wagone
Taungphila
Bawapin
Andaman Sea
Tawmoe Taung
Heinda
Putletto
Dawei
0 10 km
14°30´N
14°15´N
14°00´N
98°00´E
98°15´E
98°30´E
Biotite and two mica granite
Bt granite, Hb bt granodiorite
Quaternary sedimentary rocks
Tertiary sedimentary rocks
Mergui Group
Fault
Mine site

Fig. 5

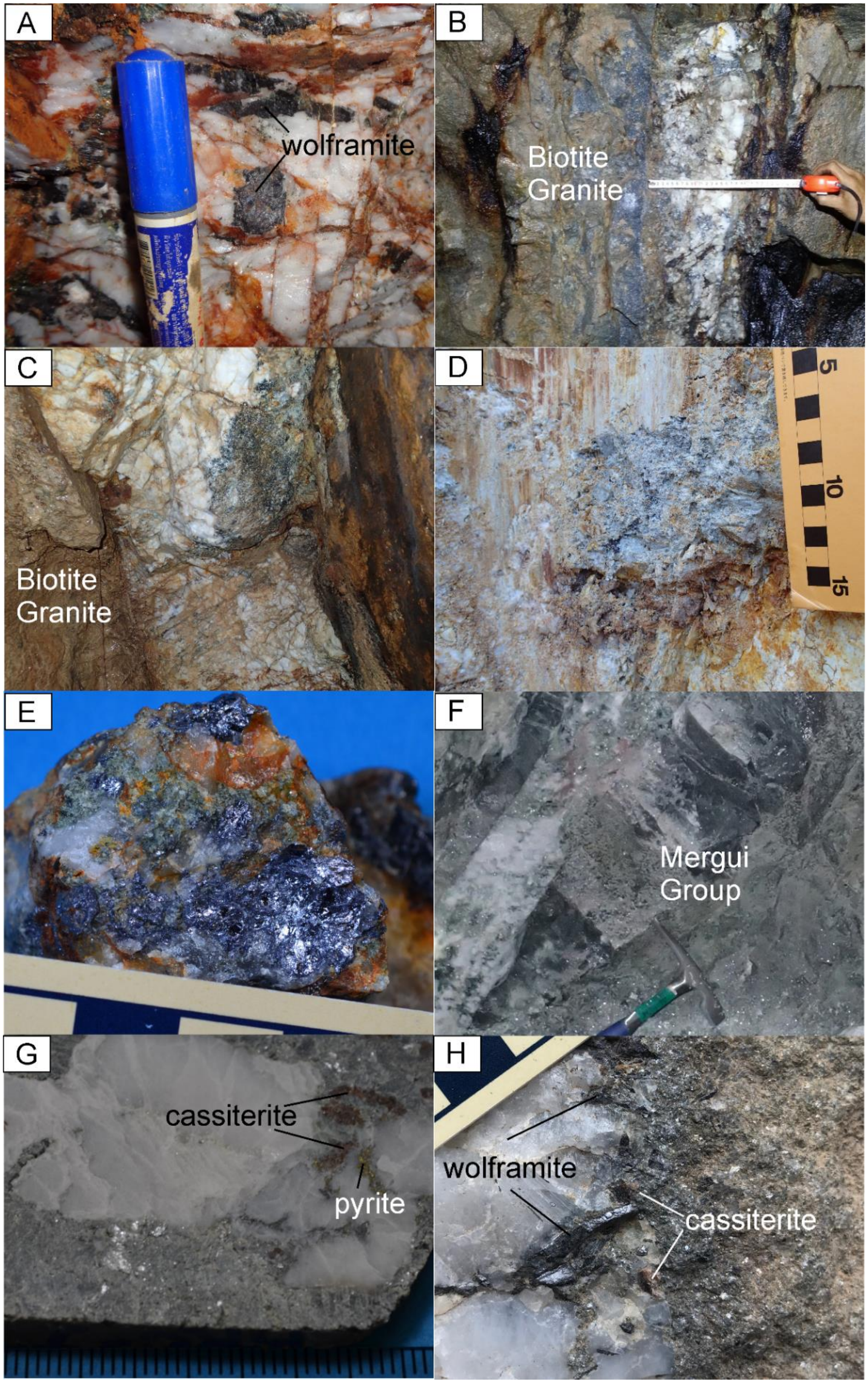
A
wolframite
B
Biotite
Granite
C
Biotite
Granite
D
5
10
15
E
F
Mergui
Group
G
cassiterite
pyrite
H
wolframite
cassiterite

Fig.6

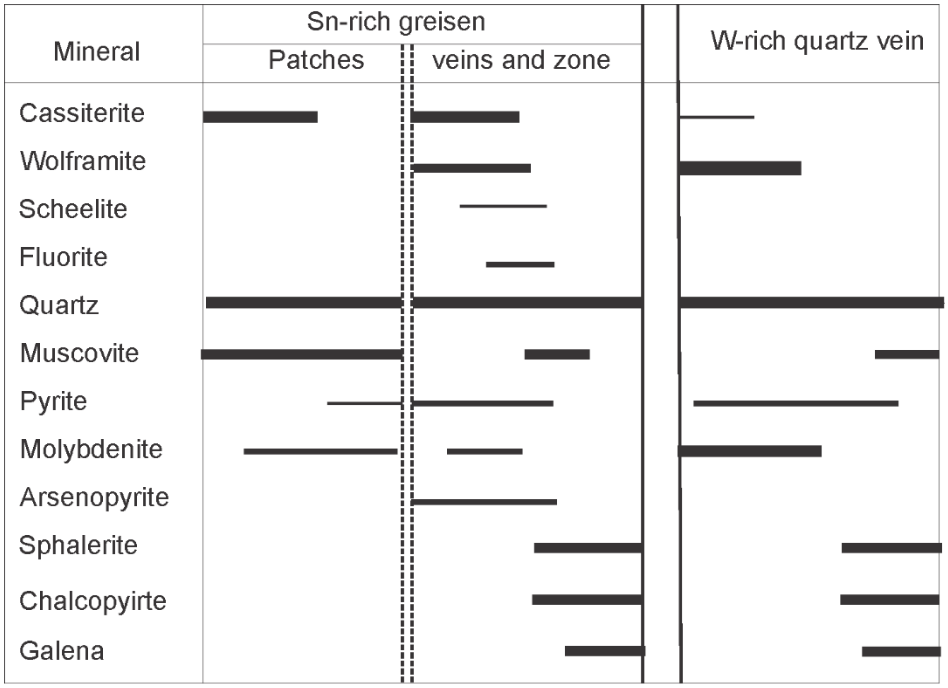
Mineral
Sn-rich greisen
Patches
veins and zone
W-rich quartz vein
Cassiterite
Wolframite
Scheelite
Fluorite
Quartz
Muscovite
Pyrite
Molybdenite
Arsenopyrite
Sphalerite
Chalcopyirte
Galena

Fig.7

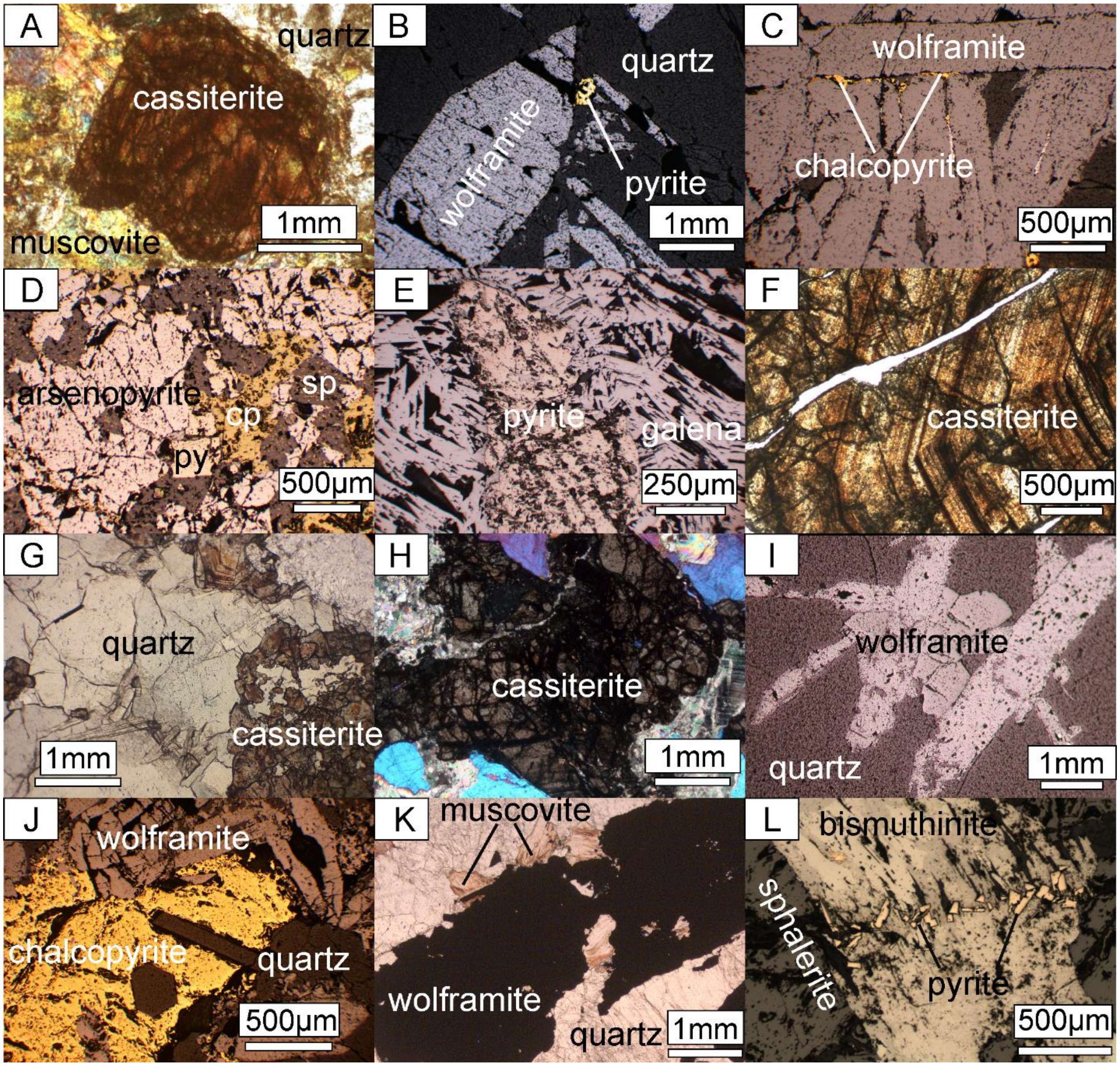
A
quartz
cassiterite
muscovite
1mm
B
quartz
wolframite
pyrite
1mm
C
wolframite
chalcopyrite
500μm
D
arsenopyrite
cp
sp
py
500μm
E
pyrite
galena
250μm
F
cassiterite
500μm
G
quartz
cassiterite
1mm
H
cassiterite
1mm
I
wolframite
quartz
1mm
J
wolframite
chalcopyrite
quartz
500μm
K
muscovite
wolframite
quartz
1mm
L
bismuthinite
sphalerite
pyrite
500μm

Fig.8

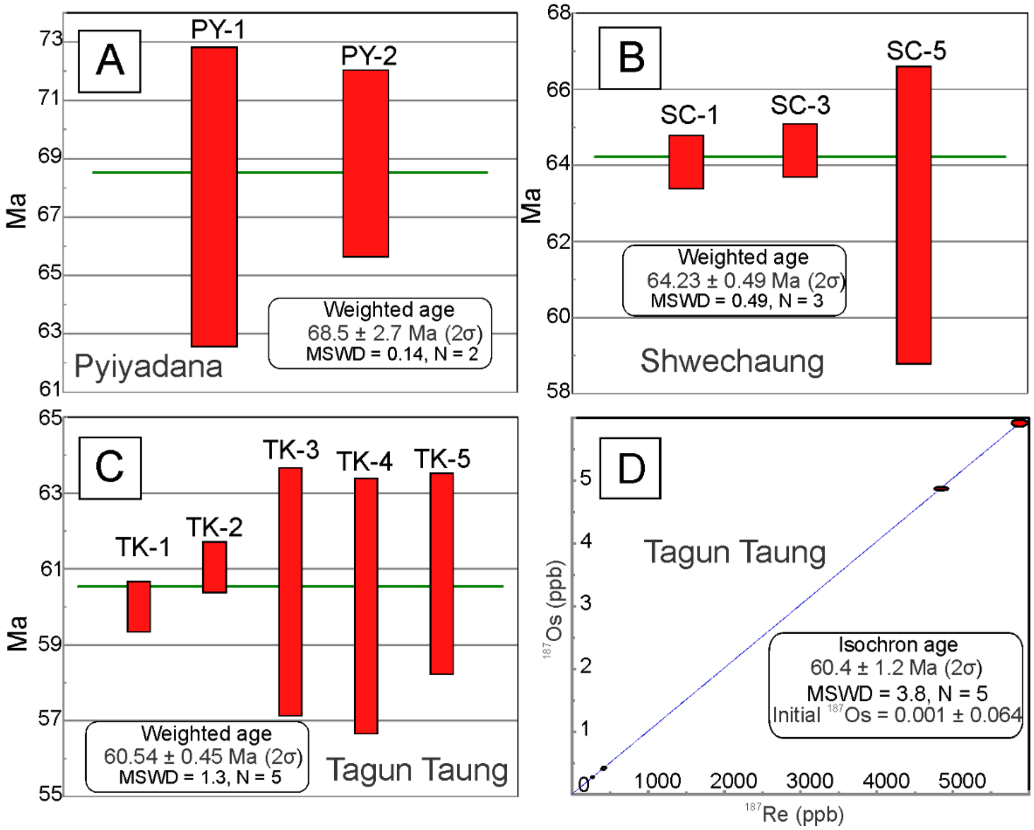

A
PY-1
PY-2
Ma
Weighted age
68.5 ± 2.7 Ma (2σ)
MSWD = 0.14, N = 2
Pyiyadana
B
SC-1
SC-3
SC-5
Weighted age
64.23 ± 0.49 Ma (2σ)
MSWD = 0.49, N = 3
Shwechaung
C
TK-1
TK-2
TK-3
TK-4
TK-5
Weighted age
60.54 ± 0.45 Ma (2σ)
MSWD = 1.3, N = 5
Tagun Taung
D
Tagun Taung
Isochron age
60.4 ± 1.2 Ma (2σ)
MSWD = 3.8, N = 5
Initial 187Os = 0.001 ± 0.064
187Os (ppb)
187Re (ppb)

Fig. 9

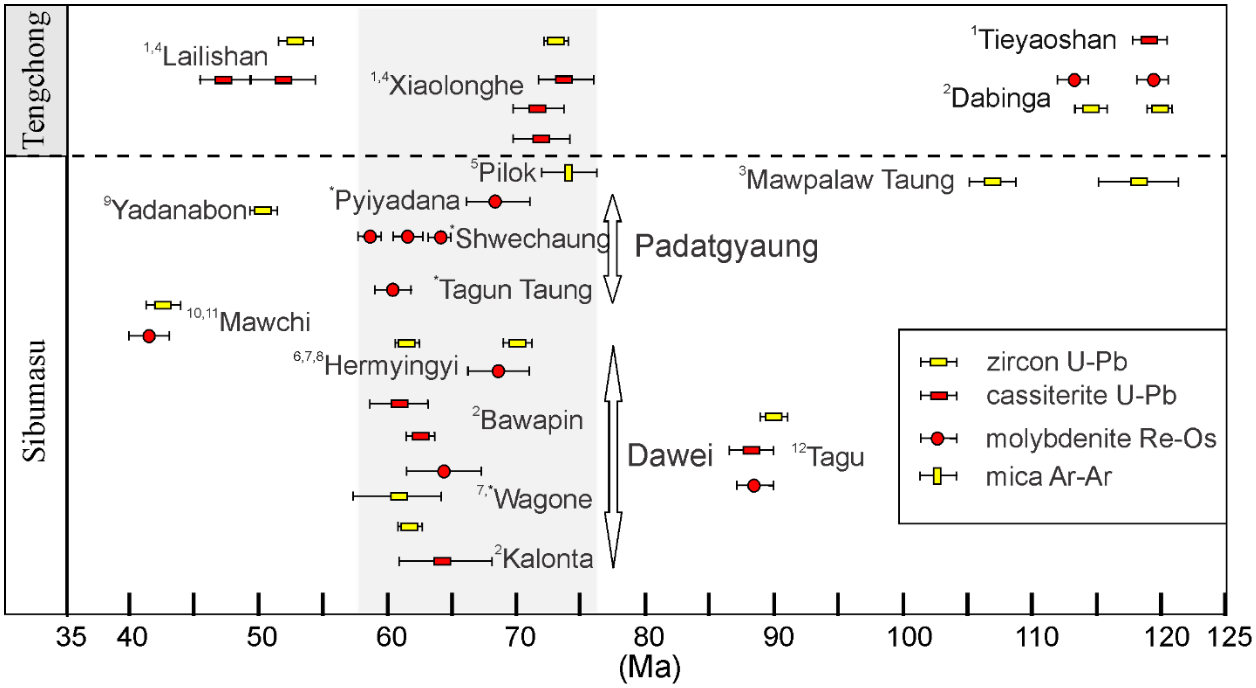
Tengchong
Sibumasu
1,4Lailishan
1,4Xiaolonghe
1Tieyaoshan
2Dabinga
5Pilok
3Mawpalaw Taung
9Yadanabon
*Pyiyadana
*Shwechaung
Padatgyaung
*Tagun Taung
10,11Mawchi
6,7,8Hermyingyi
2Bawapin
Dawei
12Tagu
7,*Wagone
2Kalonta
zircon U-Pb
cassiterite U-Pb
molybdenite Re-Os
mica Ar-Ar
35 40 50 60 70 80 90 100 110 120 125
(Ma)

Fig. 10

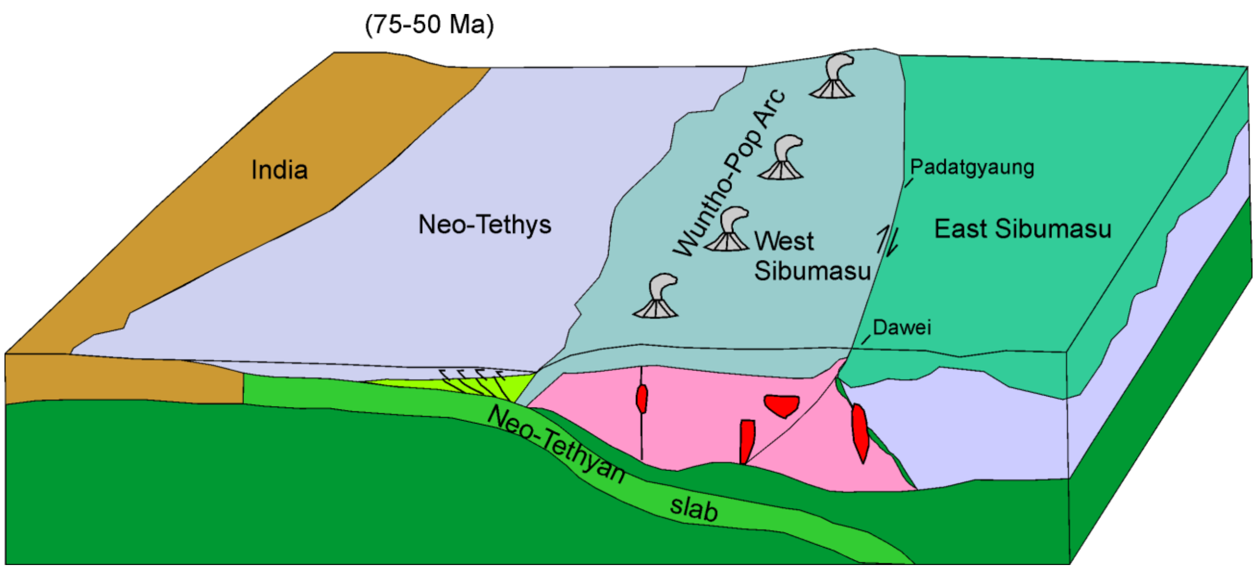
(75-50 Ma)
India
Neo-Tethys
Wuntho-Pop Arc
West Sibumasu
Padatgyaung
East Sibumasu
Dawei
Neo-Tethyan slab

Table 1 Representative EPMA results of wolframite from Padatgyaung and Dawei

	Padatgyaung										Dawei					
	Shwechaung		Sakangyi		Tagun Taung		Pyiyadana		Wagone		Kanbauk		Hermyingyi		Taungphila	
wt.%	Min	Max	Min	Max	Min	Max	Min	Max	Min	Max	Min	Max	Min	Max	Min	Max
CaO	0.00	0.00	0.00	0.00	0.00	0.00	0.00	0.00	0.00	0.00	0.00	0.02	0.00	0.01	0.00	0.03
FeO	12.78	15.70	3.82	11.31	8.04	15.23	3.18	7.66	9.91	11.89	9.37	13.04	3.01	10.36	5.24	9.56
MnO	8.72	11.89	12.31	19.51	8.47	15.33	17.69	19.92	12.96	15.99	11.26	11.60	14.20	21.26	15.04	19.08
Nb2O5	0.00	0.10	0.00	0.10	0.00	0.60	0.00	1.00	0.00	0.20	0.00	0.31	0.19	0.77	0.51	0.95
SnO2	0.00	0.01	0.00	0.03	0.00	0.01	0.00	0.05	0.02	0.22	0.00	0.04	0.00	0.11	0.03	0.17
Ta2O5	0.00	0.03	0.00	0.02	0.00	0.06	0.00	0.02	0.00	0.06	0.00	0.10	0.01	0.19	0.00	0.24
WO3	75.24	76.18	76.08	76.34	75.73	76.99	75.25	76.14	74.19	75.52	75.34	76.52	73.85	75.49	73.96	74.27
at.%																
Ca	0.00	0.00	0.00	0.00	0.00	0.00	0.00	0.00	0.00	0.00	0.00	0.00	0.00	0.00	0.00	0.00
Fe	0.55	0.66	0.16	0.48	0.34	0.65	0.14	0.32	0.41	0.51	0.40	0.56	0.13	0.44	0.22	0.40
Mn	0.37	0.57	0.53	0.84	0.36	0.65	0.75	0.86	0.56	0.68	0.48	0.64	0.61	0.91	0.64	0.82
Nb	0.00	0.00	0.00	0.00	0.00	0.01	0.00	0.02	0.00	0.01	0.00	0.01	0.00	0.02	0.01	0.02
Sn	0.00	0.00	0.00	0.00	0.00	0.00	0.00	0.00	0.00	0.00	0.00	0.00	0.00	0.00	0.00	0.00
Ta	0.00	0.00	0.00	0.00	0.00	0.00	0.00	0.00	0.00	0.00	0.00	0.00	0.00	0.00	0.00	0.00
W	0.99	1.00	1.00	1.00	0.99	1.00	0.98	1.00	0.97	1.00	0.98	0.99	0.97	0.98	0.96	0.98
Fe/(Fe+Mn)	0.52	0.64	0.16	0.48	0.34	0.64	0.14	0.30	0.38	0.48	0.38	0.54	0.13	0.42	0.21	0.39

Table 2 Molybdenite Re-Os data for Padatgyaung and Dawei

Deposit	sample	Weight (g)	Re (ppm)	± 2σ	^{187}Re (ppm)	± 2σ	^{187}Os (ppb)	± 2σ	Model Age (Ma)	± 2σ
Pyiyadana	PY-1	0.022	0.079	0.001	0.054	0.002	0.0564	0.0002	67.71	5.1
	PY-2	0.018	0.159	0.002	0.115	0.002	0.1153	0.0003	68.85	3.2
Shwechaung	SC-1	0.214	1.822	0.011	1.145	0.007	1.2242	0.0058	64.15	0.7
	SC-2	0.037	5.821	0.024	3.659	0.015	3.7546	0.0073	61.57	0.7
	SC-3	0.203	0.439	0.002	0.276	0.001	0.2961	0.0009	64.40	0.7
	SC-4	0.018	6.542	0.032	4.112	0.020	4.0252	0.0095	58.73	0.7
	SC-5	0.025	0.130	0.004	0.086	0.001	0.0862	0.0007	62.74	3.9
Tagun Taung	TK-1	0.122	9.469	0.060	5.952	0.038	5.9536	0.0205	60.01	0.7
	TK-2	0.134	7.643	0.056	4.804	0.035	4.8894	0.0110	61.06	0.7
	TK-3	0.012	0.670	0.007	0.428	0.002	0.4291	0.0080	60.41	3.3
	TK-4	0.027	0.638	0.007	0.417	0.001	0.4179	0.0079	60.03	3.4
	TK-5	0.018	0.432	0.003	0.278	0.002	0.2798	0.0038	60.89	2.6
Wagone	RO668-1	0.201	0.027	0.001	0.017	0.001	0.0180	0.0070	64.47	3.7

Table 3 Summary of the geochronological data representing the granite and associated Sn-W(-Mo) mineralization in the Western Granite Province

Granite and associated mineralization	Granite age	Associated mineralization	Deposit type	Mineralization age	Author
Tieyaoshan		Sn	greisen	119.3±1.7 Ma (cassiterite U-Pb)	Chen et al., 2014
Dabinga	120.5 ± 0.3 Ma 114.6 ± 0.6 Ma (zircon U-Pb)	Mo-W	quartz vein	119.6±1.3 Ma 113.5±1.0 Ma (Re-Os molybdenite)	Li et al., 2018b
Mawpalaw Taung	118.8 ± 2.9 Ma (zircon U-Pb)	Sn	pegmatite	106.8 ± 1.6 Ma (zircon U-Pb)	Mi Paik, 2017
Tagu (Kuntabin)	90.1 ± 0.7 Ma (zircon U-Pb)	Sn-W	quartz vein, greisen	88.1±1.9 Ma (cassiterite U-Pb) 67.7±0.5 Ma (Re-Os molybdenite)	Mao et al., 2020
Xiaolonghe	73.3 ± 0.5 Ma (zircon U-Pb)	Sn	quartz vein	71.6±2.4-71.9±2.3Ma (cassiterite U-Pb)	Chen et al., 2014, 2015
			greisen	73.9±2.0 Ma (cassiterite U-Pb)	
Pilok	72 Ma (Ar-Ar biotite)	Sn-W	pegmatite	72-76 Ma (Ar-Ar mica)	Charusiri, 1989
Hermyingyi (Dawei)	70.0±0.4 Ma 61.4±0.6 Ma (zircon U-Pb)	Sn-W-Mo	quartz vein	68.4±2.5 Ma (Re-Os molybdenite)	Jiang et al. 2017, 2019; Li et al. 2018a
Bawapin (Dawei)		Sn-W	greisen vein tin-bearing altered granite	60.7±2.5 Ma (cassiterite U-Pb) 62.5±1.0 Ma (cassiterite U-Pb)	Li et al., 2018b
Wagone (Dawei)	61.4±0.6 Ma (zircon U-Pb)	Sn	tin-bearing altered granite	60.7±3.5 Ma (zircon U-Pb)	Li et al. 2018a
		W-Mo	Quartz vein	64.5±3.7 Ma (Re-Os molybdenite)	current study
Kalonta (Dawei)				64.6±3.9 Ma (cassiterite U-Pb)	Li et al., 2018b
Pyiyadana (Padatgyaung)		Sn-W-Mo	Greisen	68.5±2.7 Ma (Re-Os molybdenite)	current study
Shwechaung (Padatgyaung)		Mo	Quartz vein	64.23±0.5 Ma 61.57±0.7 Ma 58.63±0.7 Ma (Re-Os molybdenite)	current study

Tagung Taung (Padatgyaung)		W-Mo (-Sn)	Quartz vein	60.53±1.2 Ma (Re-Os molybdenite)	current study
Lailishan	52.7 ± 0.3 – 53.0 ± 0.4 Ma (zircon U-Pb)	Sn	Quartz vein Greisen	47.4±2.0 Ma (cassiterite U-Pb) 52.0±2.7 Ma (cassiterite U-Pb)	Chen et al., 2014, 2015
Yadanabon	50.3 ± 0.6 Ma (zircon U-Pb)	Sn-W			Gardiner et al., 2016
Mawchi	42.72 ± 0.94 Ma (zircon U-Pb)	Sn-W	Quartz vein	42.4 ± 1.2 Ma (molybdenite Re-Os)	Aung Zaw Myint et al., 2017, 2018